Investigating the Effects of Acute Oxidative Stress on the Expression, Localization and Activity of Cell Death Regulatory Protein BNIP3

by

Miriam Danae Shymko

A Thesis submitted to the Faculty of Graduate Studies of The University of Manitoba in partial fulfilment of the requirements of the degree of

MASTER OF SCIENCE

Department of Biochemistry and Medical Genetics

University of Manitoba

Winnipeg, Manitoba

Abstract

BNIP3 is a BCL2 family member that promotes cell death or survival depending on expression level and localization. During hypoxia BNIP3 levels increase and localize to mitochondria, inducing autophagic cell death. Although hypoxic regions are common in solid tumors, BNIP3 expression in these cells promotes cell survival and more aggressive disease. ROS may play a role in regulating cellular response to hypoxia and is known to induce autophagy. However, BNIP3's role in regulating oxidative stress-induced cell death is unknown and the focus of this study. Effects of hydrogen peroxide exposure on expression, localization and function of BNIP3 were explored using HEK293, U87 and MEF cells. BNIP3 expression and colocalization with mitochondria increased after treatment, along with cell death. However, knockdown of BNIP3 provided minor protection, suggesting that BNIP3 is not required for cell death induced by acute oxidative stress. Overall, BNIP3 may regulate oxidative stress-induced cell death in some cells.

For my best friend.

You were with me to the end.

Acknowledgements

I would first like to acknowledge my supervisor, Dr. Spencer Gibson, and to thank him for the opportunities that being in his lab provided. I am especially thankful for his willingness to let me teach a class on his behalf. I have learned from his inspiring lectures and hope to be as good a teacher in my own future courses.

Thanks to my committee members, Dr. Tamra Werbowetski-Ogilvie and Dr. Chris Anderson, for their guidance and for challenging me to gain confidence in public speaking. I am grateful to Tamra in particular for her mentorship and encouragement.

Thanks to my cheerleading lab manager, Elizabeth Henson, for her persistent enthusiasm for my kitchen adventures, as well as for her eagerness to rejoice with me when my lab adventures went well and to give hugs and sympathy when they went poorly.

Thanks to all my lab members for teaching me so many things, and for allowing me to be the teacher sometimes. My lab has been my family for this past while and you all have a special place in my heart. Thanks especially to Yongqiang Chen for encouraging words and protocols that actually worked! And to my dear sister, Lexi Ciapala, who has been my companion, commiserator, and co-adventurer in both kitchen and lab, thanks for fighting the good fight with me. We had good times and hard times together, but every day was worth it. We grew a lot together!

Thanks to Dr. Louise Simard and to the professors in my department, institute and elsewhere for the genuine care they have shown me. I have learned so much from many of you.

Thanks to all the friends and acquaintances I have made during this journey, for joy and laughter and sometimes sorrow. I am blessed to have known each of you.

Thanks to my beloved husband, Brent, for believing in me.

Finally, thanks to the Natural Sciences and Engineering Research Council of Canada (NSERC) for the studentship funding that supported this research, and to the University of Manitoba for generous top-up funding.

Table of contents

List of Tables

List of Figures

List of Abbreviations

AIF	Apoptosis-inducing factor
AMP	Adenosine monophosphate
AMPK	5' adenosine monophosphate-activated protein kinase
AO/EB	Acridine Orange/Ethidium Bromide
ARNT	Aryl hydrocarbon receptor nuclear translocator
ATCC	American Type Culture Collection
ATP	Adenosine triphosphate
BAD	BCL2-associated agonist of cell death
BAK	BCL2 antagonist/killer
BAX	BCL2 associated X
BCA	Bicinchoninic acid assay
BCL-XL	BCL2-like 1, long version
BCL2	B-cell CLL/lymphoma 2
BH	BCL2 homology domain
BH3	BCL2 homology domain 3
BH4	BCL2 homology domain 4
BID	BH3-interacting domain death agonist
BL4	Blue fluorescence channel 4
BME	Beta-mercaptoethanol
BNIP3	BCL2/ E1B 19 kilodalton interacting protein 3
CD	Conserved domain
cDNA	Complementary DNA
CM-H2DCFDA	Chloromethyl derivative of 2',7'-dichlorodihydrofluorescein diacetate
CO_2	Carbon dioxide
CST	Cell Signaling Technology
DAPI	4',6-diamidino-2-phenylindole
DCF	CM-H2DCFDA
ddH2O	Double distilled water
DHE	Dihidroethidium
DMEM	Dulbecco's Modified Eagles Medium
DMSO	Dimethyl sulfoxide
DNA	Deoxyribonucleic acid
DR5	Death receptor 5
DRP1	Dynamin-related protein 1
ECL	Enhanced chemiluminescence
EDTA	Ethylenediaminetetraacetic acid
EGFR	Epidermal growth factor receptor
ER	Endoplasmic reticulum
ETC	Electron transport chain
FACS	Fluorescence-activated cell sorting

FBS	Fetal bovine serum
FCCP	Carbonylcyanide-4-(trifluoromethoxy)-phenylhydrazone
FL3	Fluorescence channel 3
FOXO	Forkhead box O
GAPDH	Glyceraldehyde 3-phosphate dehydrogenase
H_2	Hydrogen
H_2O_2	Hydrogen peroxide
HA-Tag	Human influenza hemagglutinin-tag
HDAC1	Histone deacetylase 1
HIF	Hypoxia inducible factor
His-Tag	Polyhistidine-tag
HRP	Horseradish peroxidase
IgG	Immunoglobulin G
KO	Knockout
LB broth	Luria-Bertani broth
LC3	Microtubule-associated protein 1A/1B-light chain 3
LIR	LC3-Interacting Region
mAb	Monoclonal antibody
MAPK	Mitogen-activated protein kinase
MCL1	Myeloid cell leukemia 1
MEF	Murine Embryonic Fibroblast
MEM	Minimum Essential Media
mM	Millimolar
MOM	Mitochondrial outer membrane
mPTP	Mitochondrial permeability transition pore
mRNA	Messenger RNA
mTOR	Mammalian target of rapamycin
mTORC1	Mammalian target of rapamycin complex 1
N_2	Nitrogen
NADPH	Nicotinamide adenine dinucleotide phosphate
NFκB	Nuclear factor kappa B
NIP1	19 kilodalton interacting protein 1
NIP2	19 kilodalton interacting protein 2
NIP3	19 kilodalton interacting protein 3
nM	Nanomolar
NOX	NADPH oxidase
NP-40	Nonidet P-40
NRT	No Reverse Transcriptase
NS	Not significant
NT	No Template
O_2	Oxygen
OMIM	Online Mendelian Inheritance in Man

OPA1	Optic atrophy 1
pAb	Polyclonal antibody
PARK2	Parkinson protein 2
PAS	Phagophore assembly site
PBS	Phosphate buffered saline
PCR	Polymerase chain reaction
PDK2	Pyruvate dehydrogenase kinase isoform 2
PE	Phosphatidylethanolamine
PEST	Proline (P), glutamine (E), serine (S) and threonine (T)
PHD2	Prolyl hydroxylase 2
PI3K	Phosphatidylinositol 3-kinase
PIP_3	Phosphatidylinositol-3-phosphate
PMSF	Phenylmethanesulfonylfluoride
PSF	PTB-associated splicing factor
PTB	Polypyrimidine tract-binding protein
PTEN	Phosphatase and tensin homolog
pVHL	von Hippel Lindau protein
qPCR	Quantitative PCR
RHEB	Ras homolog enriched in brain
RNA	Ribonucleic acid
ROS	Reactive oxygen species
RT-PCR	Reverse transcription polymerase chain reaction
SDS	Sodium dodecyl sulfate
SDS-PAGE	SDS-polyacrylamide gel electrophoresis
siRNA	Small interfering RNA
SOD	Superoxide dismutase
STAT3	Signal transducer and activator of transcription 3
TBS	Tris buffered saline
TBS-T	Tris buffered saline with Tween 20
TM	Transmembrane
TMRM	Tetramethylrhodamine, methyl ester
TNBC	Triple negative breast cancer
TP53	Tumour protein 53
ULK1/2	UNC-51-like kinases 1 and 2
µM	Micromolar
USA	United States of America
VDAC	Voltage dependent anion channel
WT	Wild-type
ΔTM	Transmembrane deleted

Chapter 1: Introduction

1.1 Overview of the thesis

Although a considerable amount of research has been conducted looking into the effects of hypoxia on the expression, localization and activity of the cell death regulatory protein BNIP3, comparatively little is known about the effects of other stressors. As I will describe later in this thesis, BNIP3 has been found to contribute to poor outcomes in patients with a variety of cancer types including glioblastoma, the most aggressive form of adult brain cancer. While it is possible that hypoxia alone is sufficient to induce BNIP3-mediated cancer survival and chemotherapy resistance, is that really the full story?

Mounting evidence in the literature suggests that oxidative stress, which is very common in cancer, plays a role in hypoxia-induced stabilization of HIF1α, a transcription factor known to upregulate *BNIP3*. Oxidative stress has also been implicated in activation of other transcription factors involved in *BNIP3* upregulation, and in activation of autophagy, a cell survival process that is one of the defining features of BNIP3. Could oxidative stress in fact be a main contributor to BNIP3's status as a poor prognosis marker?

In this study I sought to determine the role of acute oxidative stress on the expression, localization and activity of BNIP3. Using the human embryonic kidney cell line HEK293 and the human glioblastoma cell line U87 and inducing oxidative stress with hydrogen peroxide, I measured changes in BNIP3 protein levels by western blot, mRNA levels by qRT-PCR, and localization by immunofluorescence microscopy. I also assessed changes in total cell death by microscopy and flow cytometry, with hydrogen peroxide

treatment and with or without knockdown of BNIP3. As a complementary approach, I evaluated total cell death with hydrogen peroxide treatment in murine embryonic fibroblasts that were either wild type or knockout for BNIP3.

Acute oxidative stress caused an increase in BNIP3 expression levels and mitochondrial localization in HEK293 cells but not in U87 cells, while loss of BNIP3 provided some protection against cell death in siRNA-transfected HEK293 cells and *BNIP3*-knockout murine embryonic fibroblasts but did not completely prevent cell death. These results suggest that BNIP3 may contribute in some cell types to death caused by acute oxidative stress, but is not required for it. BNIP3 does not appear to play a role in acute oxidative stress-induced cell death (or survival during acute oxidative stress) in U87 cells. However, there is sufficient evidence to warrant exploration of the effects of chronic oxidative stress on the expression, localization and activity of BNIP3, as that is more physiologically relevant in a cancer setting.

1.2 BCL2 family of apoptosis regulators

Death is the ultimate fate of all organisms, and the cells that comprise them. Although living beings have an inherent drive to survive, cells may initiate death programs in response to a variety of stressors or simply as part of the normal course of development[1–3]. The process of cell death is tightly controlled in order to prevent an untimely or inappropriate demise, especially when cells experience damage that can be repaired or temporary stress that can be resolved. However, cells must be able to die when necessary and may do so by inducing apoptosis, a type of programmed cell death that is characterized by such morphological features as condensation of the nucleus,

fragmentation of DNA, blebbing of the plasma membrane, and cell shrinkage followed by packaging into vesicles for degradation[4,5]. These events can occur as a result of permeabilization of the mitochondrial outer membrane (MOM) leading to release of cytochrome c and other pro-apoptotic proteins, and cleavage of caspases that act as executioners of the cell death program[1,5–7].

A key set of regulators involved in this process is the B-cell CLL/lymphoma 2 (BCL2) family of proteins, which play both direct and indirect roles in mediating apoptosis. Members of this large family act primarily at intracellular membranes and can be broadly categorized into three groups: 1) Multi-domain pro-survival family members such as BCL2 and myeloid cell leukemia 1 (MCL1); 2) Multi-domain pro-apoptotic family members such as BCL2 associated X (BAX) and BCL2 antagonist/killer (BAK); and 3) BH3 domain-only family members such as BH3-interacting domain death agonist (BID) and BCL2-associated agonist of cell death (BAD), which are also pro-apoptotic[5,7,8]. BCL2 has four BCL2 homology (BH) domains that are present in other family members. Multi-domain family members have all four BH domains, with a modified BH4 domain in pro-apoptotic members, while BH3-only family members have only the BH3 domain, which is essential for heterodimerization with other family members[1,5,7].

Interactions between BCL2 family members determine whether apoptosis is initiated or repressed. Apoptosis can be induced by extracellular signals via the extrinsic pathway of apoptosis or by intracellular signals via the intrinsic pathway, but both pathways converge at mitochondria and are influenced by the activity of BCL2 family members[1,5]. Although a variety of models of BCL2 family member interaction have been developed, the exact process and functionality have yet to be determined. One model

proposes that BH3-only proteins displace pro-survival proteins by binding to pro-apoptotic proteins, while other models suggest different ways that pro-survival proteins sequester BH3-only proteins to prevent activation of pro-apoptotic proteins[1,5,8]. What has been determined is that BH3-only BCL2 proteins respond to intracellular stress signals to directly or indirectly activate the pro-apoptotic BCL2 proteins BAX and BAK, which form oligomers in the MOM to permeabilize the membrane and allow release of cytochrome c, while pro-survival BCL2 family members repress apoptosis by inhibiting both anti-apoptotic and BH3-only family members[1,5,8].

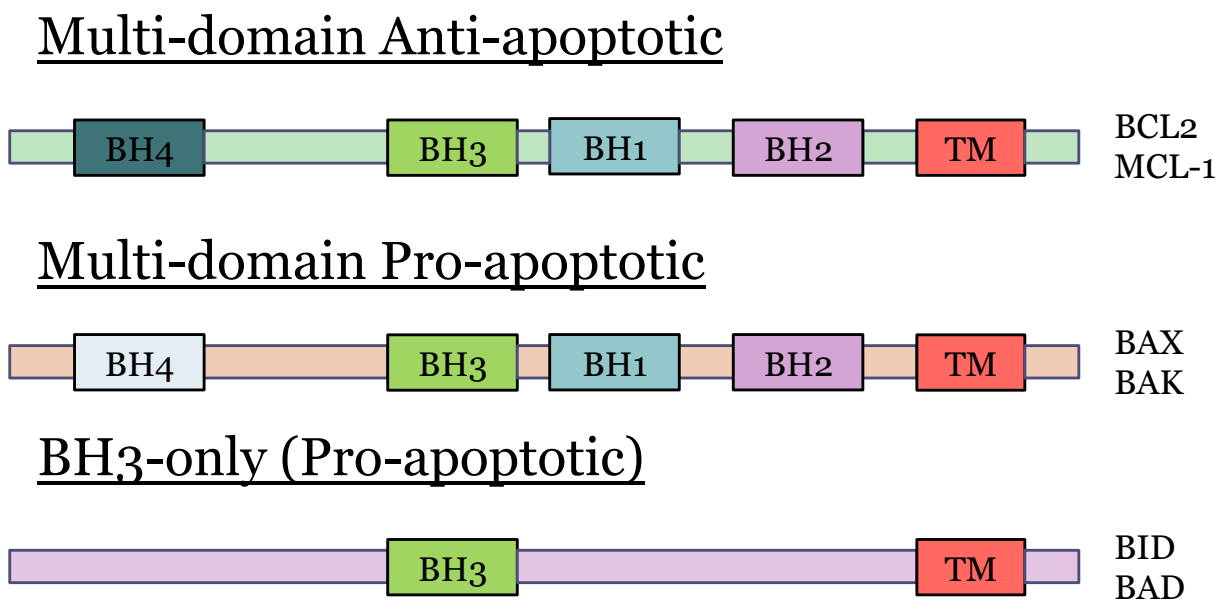

Figure 2: BCL2 family of cell death regulators and its subfamilies. The BCL2 family of proteins is comprised of three subfamilies, with each playing an important role in regulating cell death. Multi-domain anti-apoptotic proteins have all four BCL2 homology (BH) domains and block the activity of pro-apoptotic family members. Multi-domain pro-apoptotic proteins have three BH domains and a modified BH4 domain. These proteins permeabilize the mitochondrial membrane to effect death in response to stress-sensing BH3-only family members, which are typically pro-apoptotic.

BH3-only proteins are important stress-sensors that regulate cell death. The following sections will describe the features and functions of the BH3-only protein BNIP3, which is the focus of this thesis.

1.3 BNIP3 History

BCL2/ E1B 19 kilodalton interacting protein 3 (BNIP3) is one of three proteins identified in the early 1990s by a yeast two-hybrid screen for proteins that interact with the adenovirus E1B 19kDa protein[9], a viral homolog that is functionally equivalent to the pro-survival protein BCL2[9,10]. The E1B gene can be transcribed into two different sized proteins, one 19 kilodaltons in size and the other 55 kilodaltons in size, with the smaller protein acting as an apoptosis-inhibiting protein equivalent to BCL2[11,12]. This protein is utilized by adenovirus to turn off cellular responses to invasion that would otherwise cause apoptosis in the invaded host cell.

As the mechanism of action for E1B and BCL2 were unknown at the time, researchers sought to uncover the mechanism by identifying interaction partners that may play a role in promoting cell death. Boyd et al used a yeast two-hybrid screen and cloning methods to identify NIP1, NIP2, and NIP3 as proteins that interact with both E1B 19K and BCL2[9]. Of the three proteins, NIP3 (later renamed BNIP3) alone was shown to localize to mitochondria. More than two decades of research into the function of this protein has revealed that it has a variety of functions, playing roles in cell death, cell survival, and autophagy, a form of self-digestion. The functions of BNIP3 will be discussed in detail in a later section.

1.4 BNIP3 Structure

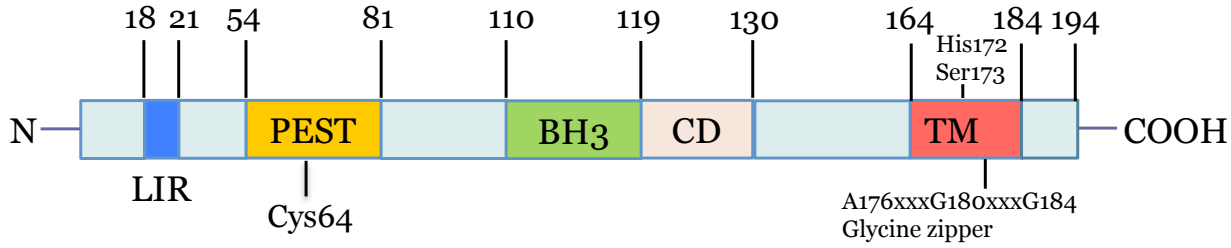

Figure 3: BNIP3 protein structure. BNIP3 has five notable regions. 1) An LC3-Interacting Region (LIR) that interacts with LC3 proteins studding autophagosomes to allow docking of these structures and subsequent engulfment of mitochondria for digestion. 2) A serine/threonine rich PEST domain associated with rapid turnover of proteins. A conserved cysteine residue (Cys64) is easily oxidized and contributes to dimer stability. 3) A BCL2 Homology 3 (BH3) that allows interaction with BCL2 family members but is not required for BNIP3's function. 4) A conserved domain (CD) that has no known function. 5) A transmembrane domain (TM) that is essential for homodimerization and mitochondrial localization, both of which are necessary for BNIP3's cell death function. A histidine-serine node (His172, Ser173) and a glycine zipper tandem to a GxxxG motif contribute greatly to dimer stability.

While the *BNIP3* gene was initially identified as being located on human chromosome 14q11.2–q12, based on radiation hybrid mapping[13], it is now thought to be located at 10q26.3 according to the OMIM (Online Mendelian Inheritance in Man) database, based on mapping of the gene sequence to the genomic sequence contained in the database[14]. The gene contains six exons[15] and encodes a protein 194 amino acids in length[9,16]. Although BNIP3's predicted molecular weight is 21.54 kilodaltons, BNIP3 migrates on SDS-PAGE gels as a band at 30 kilodaltons and a band at 60 kilodaltons, with the larger band attributed to homodimerization[16,17]. The homodimer is resistant to disruption from both reducing conditions and SDS detergent[16,18], as BNIP3 has many features that promote dimer stability. Most of these features are located in BNIP3's

transmembrane domain (TM), comprised of amino acids 164-184 near the carboxy-terminal of the protein[19]. The transmembrane domain is essential for targeting BNIP3 to mitochondria, homodimerization, heterodimerization with BCL2 and BCL-X_L, and for performance of its cell death function[20–24]. These critical activities are mediated by a variety of structural features within the domain.

BNIP3's transmembrane domain is a right-handed alpha-helix[23,25] with a $A^{176}xxxG^{180}xxxG^{184}$ (glycine zipper tandem to a GxxxG) motif providing an interface for helix-helix interactions in the form of intermonomer hydrogen bonding between polar side chain residues His^{173} and Ser^{172} as well as other polar side chain and backbone residues[18,19,22,23]. These helix-helix interactions remain stable even when the dimer is associated with membranes or is in the presence of detergents[18,25,26]. BNIP3 is targeted to mitochondria and the dimer inserts into the outer mitochondrial membrane, where His^{173} and Ser^{172} form a His-Ser node in the middle of the intermembrane space[25]. The residues in the node form both intermonomeric hydrogen bonds with each other and intramonomeric hydrogen bonds with Leu^{169} and Ser^{168} carbonyl groups. This hydrophilic motif is accessible to water and increases permeability of water into the mitochondrial membrane, subsequently making ion conductance possible. Accessibility to water increases considerably upon protonation of one or both His^{173} residues. Next to the transmembrane domain, N-terminal side aromatic rings Phe^{157}, Phe^{161}, and Phe^{165} form an intermonomeric hydrophobic cluster that contribute weakly to dimer stability and may modulate membrane permeability to water.

Other important contributors to dimer stability include a cysteine residue at the N-terminal domain, which is conserved across species[19,27]. Cys^{64} projects outward facing the

cytosol, allowing it to be easily oxidized to form intermonomer cysteine bonds[27]. Mutation of this residue has been found to reduce homodimer formation and affect BNIP3's ability to induce both apoptosis[27] and autophagy[28]. Overall, many structural features work together to form the strong, stable dimers necessary for BNIP3 to function.

One function of BNIP3 involves induction of cell death via interactions with BCL2 and its homologs. BNIP3 has a BCL2 homology 3 (BH3) domain[20] but none of the other BH domains, making it a member of the BH3-only subfamily of BCL2 proteins. While most members of this subfamily have a pro-death function that is critically dependent on their BH3 domain allowing heterodimerization with anti-apoptotic proteins[7,20], BNIP3 has an atypical BH3 domain that is not necessary for heterodimerization or cell death induction[21,29,30]. Replacing the BH3 domain of pro-apoptotic BCL2 family member BAX with the BH3 domain of BNIP3 demonstrates that this domain plays a functional pro-apoptotic role in BAX[20], but seemingly not a significant role in BNIP3. Instead, BNIP3's TM and N-terminal domains are both essential for interaction with BCL2 and either domain is individually sufficient for heterodimerization with the BCL2 homolog BCL-X_L to occur[21]. Deletion of the BH3 domain does not abrogate BNIP3's ability to interact with BCL2 family members or induce cell death[21,24,29]. However, the BH3 domain appears to be required for growth factor mediated protection against BNIP3-induced cell death[31].

Deletion of the conserved domain (CD) immediately adjacent to the BH3 domain also does not affect the activity of BNIP3[21,30]. This domain has a high degree of sequence similarity between the human and C. elegans versions of the protein, but as of yet has no known function[21,30]. Other notable features of the BNIP3 protein include a serine-rich PEST domain at residues 54-81[16,32,33] and a LC3-Interacting Region (LIR) at residues 18-21[34] in

the N-terminal region. PEST domains are regions that contain unusually high frequencies of proline (P), glutamine (E), serine (S) and threonine (T) residues flanked by positively charged amino acid residues[16,33,35]. These sequences are associated with rapid degradation of proteins by the proteasome[16,35], but no clear link has yet been established between BNIP3's PEST domain and its degradation[17]. BNIP3's LIR sequence allows BNIP3 to act as a docking site for microtubule associated protein 1 light chain 3 (LC3) proteins on autophagosomes, thereby promoting engulfment of mitochondria and endoplasmic reticula for degradation via autophagy[28,34,36]. Hence, this short sequence holds a key to one of BNIP3's several functions.

1.5 BNIP3 Function

Although BNIP3 mediates a delayed and less potent induction of cell death than other BCL2 family members[20,30,37,38], it has been observed to induce mitochondrial dysfunction and a number of different cell death types, including apoptosis, necrosis, and autophagic cell death, with the type of cell death depending on cell type. It has also been shown to promote cell survival in a number of ways. This section will describe the different functions of BNIP3.

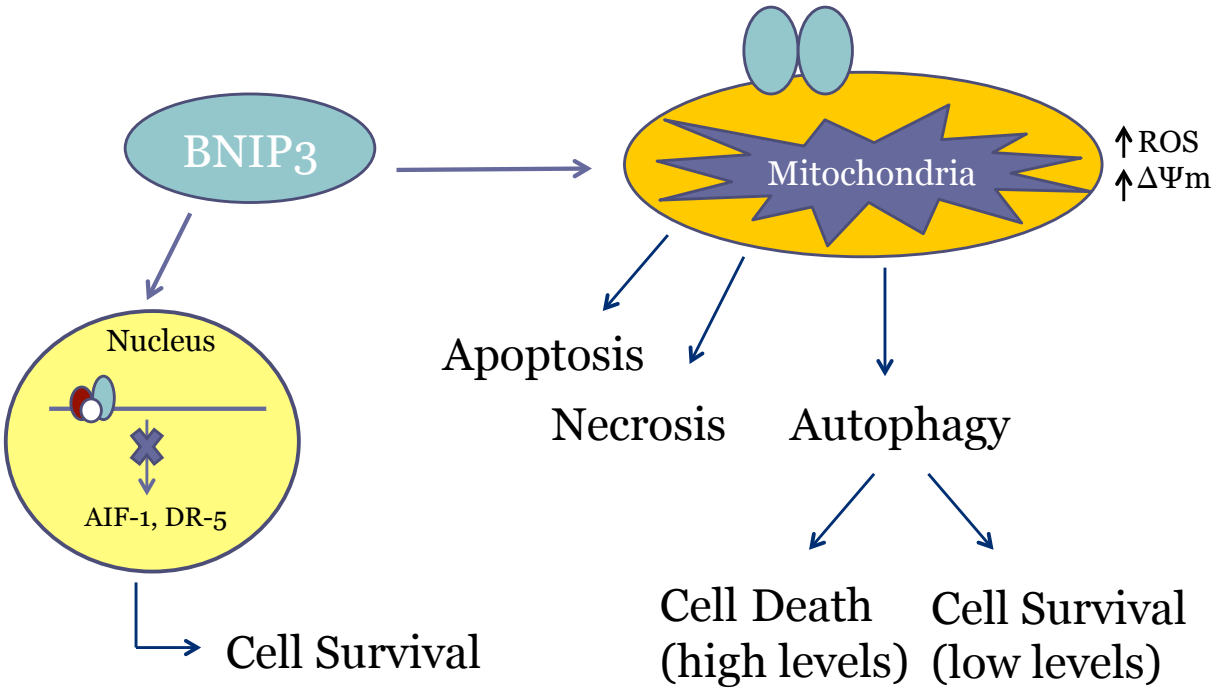

Figure 4: BNIP3 function depends on localization and expression levels. BNIP3 typically localizes to mitochondria. Here, low levels of BNIP3 expression promote survival via autophagy by recycling damaged proteins and organelles for resources cells can use to survive, while high levels of expression can cause cell death by apoptosis (Programmed Cell Death Type I), necrosis, or autophagic cell death (Programmed Cell Death Type II). Alternatively, BNIP3 can localize to the nucleus, where it participates in a transcriptional repression complex that blocks production of the pro-apoptotic proteins Apoptosis Inducing Factor (AIF) and Death Receptor 5 (DR-5). This in turn promotes survival. A splice variant of BNIP3 lacking the transmembrane domain is unable to localize to mitochondria

1.5.1 BNIP3-mediated mitochondrial dysfunction

BNIP3 plays a key role in regulating mitochondrial function and number[39,40]. Increased expression of BNIP3 leads to mitochondrial swelling and fragmentation, loss of mitochondrial membrane potential and subsequently ATP production, and increased production of reactive oxygen species[37,41–44]. Once the BNIP3 dimer inserts into the outer mitochondrial membrane, the C-terminal domains interact with optic atrophy 1 (OPA1), a dynamin protein responsible for both mitochondrial fusion and sequestering of

cytochrome c[42,45]. This interaction occurs in the intermembrane space, where BNIP3 inhibits the fusion activity of OPA1 oligomers. Meanwhile, the N-terminal domains interact with dynamin-related protein 1 (DRP1), a mitochondrial fission protein located in the cytosol[42,46]. These events lead to mitochondrial dysfunction, as detailed above. Dysfunctional mitochondria are cleared by autophagy, but can also lead to cell death if damage is excessive[36,43,44].

1.5.2 BNIP3-mediated cell death

BNIP3 induces apoptosis via pro-apoptotic BCL2 family members BAX and BAK, possibly as downstream effectors of interactions between BNIP3 and BCL2 or BCL-X_L[45,47], although BNIP3 has been observed to form heterodimers with BAX in the outer mitochondrial membrane of cardiomyocytes[48]. These interactions lead to opening of the mitochondrial membrane permeability transition pore (mPTP) in many cell types[29,44,47], but may also induce membrane permeabilization independent of the mPTP[41,49].

Furthermore, the type of death induced by BNIP3 is dependent on cell type. In neuronal cells BNIP3 interacts with the voltage dependent anion channel (VDAC) to release endonuclease G, leading to a caspase-independent form of cell death without cytochrome c release or caspase cleavage[50,51], while in cardiomyocytes BNIP3-mediates mitochondrial membrane permeabilization (with or without opening of the mPTP) and release of cytochrome c, leading to classical caspase-dependent apoptosis[41,44,47,48]. Meanwhile, cells of epithelial origin have been shown to experience a necrotic-like caspase-independent cell death without release of any mitochondrial proteins, including cytochrome C and

endonuclease G[29,31,52]. In other contexts, cells may die from excessive autophagy, or autophagic cell death[53–56].

Apoptosis	Necrosis	Autophagic cell death
Nuclear condensation	Nuclear dilation	Minor nuclear changes
Chromatin condensation	Some chromatin condensation	Some chromatin condensation
Membrane blebbing	Membrane rupture	Membrane rupture
Cell shrinkage	Cell swelling	Organelle swelling
Cell fragmentation and packaging	Total cell lysis – no packaging	Autophagosomes present

Table 1: The three main types of cell death and their morphological characteristics. Apoptosis is also known as Programmed Cell Death Type I, while autophagic cell death is also known as Programmed Cell Death Type II. Autophagic cell death shares some features with necrosis, which may be regulated or unregulated.

1.5.3 BNIP3-mediated autophagy

As mentioned, BNIP3 plays a key role in regulating mitochondrial function and number. Mitochondrial dysfunction may lead to cell death, but first and foremost leads to mitochondrial autophagy (mitophagy). BNIP3-mediated autophagy stimulates turnover of mitochondria and promotes survival, while blockage of autophagy leads to necrotic cell death[36,37,40], indicating that autophagy plays an important role in regulating cell survival. Autophagy is a form of self-digestion that recycles damaged proteins and organelles to produce needed resources such as ATP and amino acid building blocks[37,57,58]. This is an essential process that occurs constitutively at basal levels as part of cellular homeostasis, but it can also be utilized at higher levels to endure times of nutrient and energy stress.

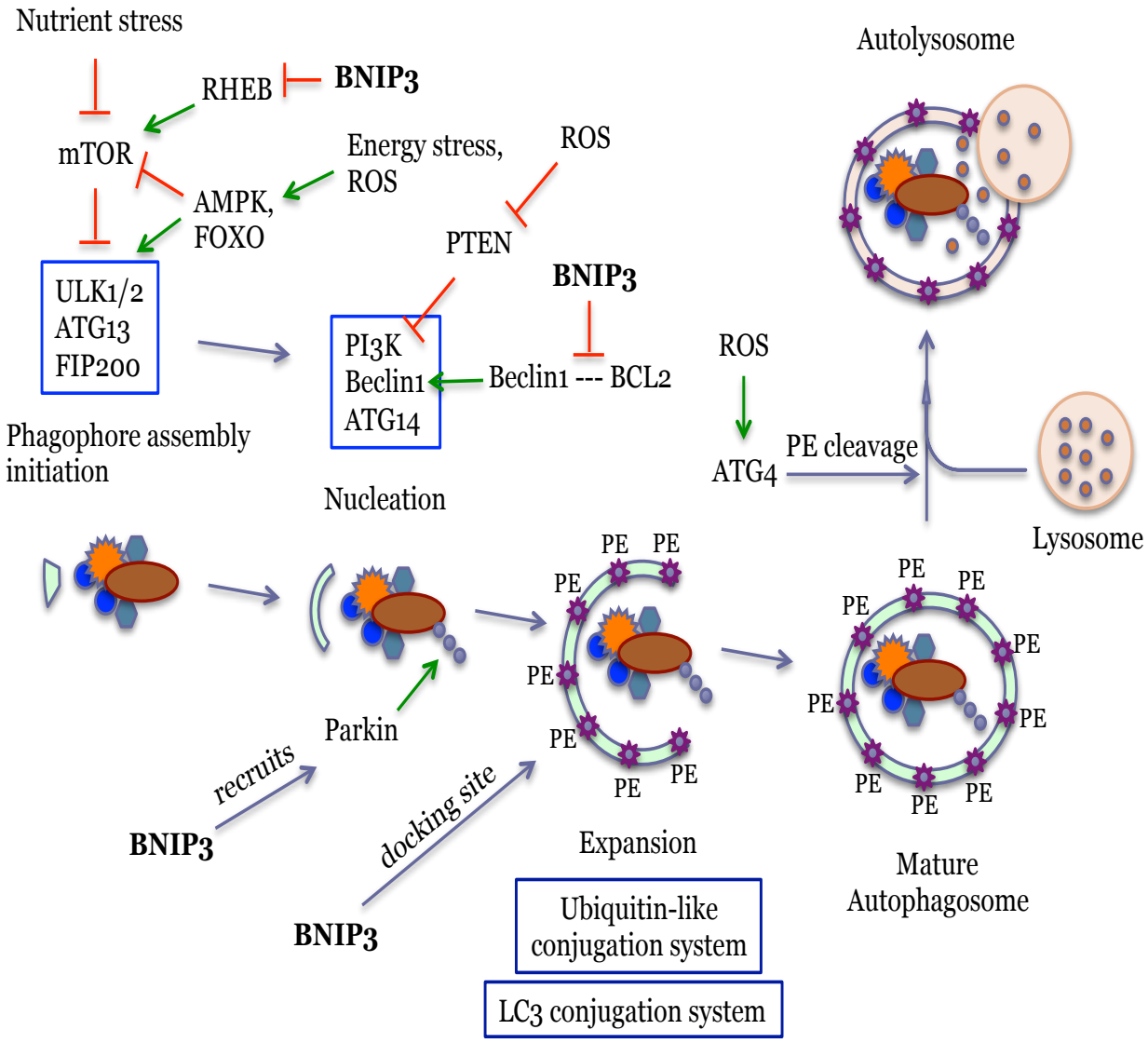

Figure 5: Macro-autophagy initiation and process. Macro-autophagy begins with initiation of phagophore assembly, which is regulated by mTOR, a kinase that phosphorylates ULK1/2 to inhibit its activity. AMPK can directly or indirectly activate autophagy via interaction with ULK1/2 or with mTOR. Once phagophore assembly has begun, the ULK complex recruits autophagy proteins for nucleation of the phagophore. BNIP3 recruits the E3 ubiquitin ligase Parkin to ubiquitinate mitochondria, leading to phagophore formation around the organelle. A PI3K complex produces lipids needed to recruit further autophagy proteins for expansion of the phagophore and studding with LC3 proteins conjugated to phosphatidylethanolamine (PE). BNIP3 interacts with these LC3 proteins to allow engulfment of mitochondria. PE is then cleaved from LC3 and the mature autophagosome fuses with a lysosome to form an autolysosome that degrades the engulfed contents.

There are three known types of autophagy: 1) Chaperone-mediated autophagy, wherein chaperone proteins selectively transport specific proteins directly to lysosomes for degradation; 2) Micro-autophagy, wherein small cytoplasmic cargo enter lysosomes directly via invaginations in the lysosomal membrane; 3) and Macro-autophagy, wherein a double-membrane vesicle called an autophagosome engulfs cytoplasmic proteins and organelles before fusing with a lysosome for delivery and degradation of the contents[58]. BNIP3 plays a significant role in macro-autophagy (hereafter referred to as "autophagy"), which is also the better-studied process of the three types and will be described in this section.

Cellular stress produces signals that lead to assembly of an autophagy protein complex consisting of UNC-51-like kinases 1 and 2 (ULK1/2) and several other autophagy proteins, at the phagophore assembly site (PAS)[57,58]. The complex acts as a scaffold for recruiting autophagy proteins to this site. Nutrient stress signalling occurs through inhibition of the mammalian target of rapamycin complex 1 (mTORC1), an amino acid sensor that inactivates the ULK1/2 complex via phosphorylation when nutrients are abundant[57–59]. BNIP3 has been shown to directly inhibit RHEB, an upstream activator of mTORC1[49,60]. Energy stress signalling occurs through 5' adenosine monophosphate-activated protein kinase (AMPK), an energy sensor that indirectly inhibits mTORC1 when levels of AMP in the cell are much higher than levels of ATP, although transcription factor FOXO-mediated inhibition of mTOR can also occur[57,58,61].

Once phagophore assembly has been initiated, a complex consisting of class III phosphatidylinositol 3-kinase (PI3K), the BH3-only protein BECN1 (more commonly called Beclin1), and other autophagy proteins, is recruited to the PAS for nucleation of the

phagophore, an important process whereby PI3K produces phosphatidylinositol-3-phosphate (PIP_3) to further recruit more autophagy proteins and allow completion of the phagophore to occur[57–59]. BECN1 is sequestered in complexes with BCL2 tethered to endoplasmic reticulum (ER), but binding of BNIP3 to BCL2 disrupts these complexes and frees BECN1 to participate in autophagy[30,62,63]. Irreversible conjugation of ubiquitin-like autophagy proteins elongate the phagophore through formation of complexes, which are then conjugated to LC3 bound to phosphatidylethanolamine (PE)[57,58]. Mitochondrial BNIP3 interacts with LC3 via its LC3-interacting region (LIR), enabling targeting of the phagophore to mitochondria for mitophagy[34,58,64]. BNIP3 also recruits the E3 ubiquitin ligase Parkin (encoded by *PARK2*) to mitochondria, where it ubiquitinates mitochondrial proteins, leading to phagophore formation around the ubiquitinated mitochondria[46,65,66].

Completion of phagophore elongation produces a mature autophagosome with contents sequestered from the cytosol. This autophagosome then fuses with either a lysosome or an endosome after cleavage of PE from LC3, creating an autolysosome that degrades the sequestered contents and subsequently releases the recycled materials into the cytoplasm[57,58].

1.5.4 BNIP3-mediated transcriptional repression

BNIP3 lacks a nuclear localization signal, but is able to localize to the nucleus of glial cells and of human gliomas[33,67]. How BNIP3 localizes to the nucleus is unknown, but nuclear BNIP3 has been shown to participate in a transcriptional repression complex that also includes histone deacetylase 1 (HDAC1) and polypyrimidine tract-binding protein (PTB)-associated splicing factor (PSF), blocking transcription of apoptosis-inducing factor

(AIF) and death receptor 5 (DR5)[68,69]. This promotes cell survival and contributes to chemotherapy resistance in gliomas.

1.6 BNIP3 Regulation

Since BNIP3 is able to regulate cell survival in so many ways, modulation of its activity and levels in cells is essential for preventing excessive or inappropriate activation. This section will describe regulation of BNIP3 at the protein and gene level.

1.6.1 BNIP3 degradation

BNIP3's possible degradation by the proteasome has already been discussed in an earlier section. In brief, BNIP3 has a PEST domain that likely targets it for ubiquitination and proteasomal degradation, but the players involved have yet to be identified[17]. Another method of BNIP3 turnover is via ULK1-mediated autophagy, which has been shown to reduce BNIP3 levels in cells experiencing both hypoxia and nutrient starvation[32]. Mitochondrial localization of BNIP3 is not required for this autophagy-related reduction to occur.

1.6.2 BNIP3 phosphorylation

BNIP3 has a number of phosphorylation sites that have been shown to modulate its activity. Phosphorylation of serine residues on either side of the LC3-interacting region in the N-terminal domain leads to increased interaction between BNIP3 and LC3 and promotes mitophagy[34]. In contrast, phosphorylation of serine/threonine residues in the C-terminal tail prevents mitochondrial dysfunction and cell death, but not autophagy, by blocking the interaction between BNIP3 and OPA1[42]. As such, BNIP3's phosphorylation state can determine whether it is more likely to promote autophagy or cell death.

1.6.3 BNIP3 alternative splicing

Which form of BNIP3 is expressed in cells can also affect survival outcomes. Alternative splicing of *BNIP3* removes exon 3 from the mRNA, which creates a stop codon at the junction between exons 2 and 4, thereby producing a truncated protein comprised mainly of the N-terminal domain[70]. This truncated protein does not localize to mitochondria as it lacks the transmembrane domain, but instead acts as a dominant negative against full-length BNIP3 and blocks its cell death function[15,33,70]. Human cancer cells preferentially express spliced BNIP3 over full length-BNIP3, and pyruvate dehydrogenase kinase isoform 2 (PDK2), an enzyme involved in glycolysis that is upregulated in many cancers, has been shown to mediate alternative splicing of *BNIP3* by an unknown mechanism[15].

1.6.4 BNIP3 transcriptional upregulation by HIF1

BNIP3 has some level of expression in most tissues of the body[71,72], and in particular is present at basal levels in skeletal muscle, the heart, and the nucleus of glial cells[33,67,73,74]. A variety of stress conditions are known to dramatically increase BNIP3 expression. Importantly, low oxygen conditions (hypoxia) have been well established to upregulate BNIP3 expression[31,60,72,74,75]. Normally oxygen levels are maintained at around 5-10% in cells as oxygen is the final electron acceptor for the mitochondrial electron transport chain and is therefore essential for mitochondrial production of cellular energy, ATP[76–78]. When oxygen levels decrease, cells must act swiftly to ensure a sufficient supply of oxygen and energy are available for survival.

A key factor in this process is the transcription factor hypoxia inducible factor 1 (HIF1), comprised of two subunits: an α subunit responsible for promoter activation, and a β subunit that is an aryl hydrocarbon receptor nuclear translocator (ARNT) responsible for nuclear localization of the transcription factor[75,76]. Both subunits are constitutively expressed, but the alpha subunit is rapidly degraded during normal oxygen conditions (normoxia) due to hydroxylation by the HIF-specific prolyl hydroxylase enzyme PHD2 and subsequent recognition and ubiquitination by the von Hippel Lindau protein (pVHL) component of an E3 ubiquitin ligase, leading to degradation by the proteasome[76,79]. Hypoxia leads to inhibition of the activity of PHD2, allowing HIF1α levels to stabilize and the α and β subunits to come together as a complete transcription factor. HIF1 subsequently activates transcription of a number of hypoxia inducible genes, including *BNIP3* and other genes involved in angiogenesis, migration, and metabolic adaptation, via HIF-responsive elements in the gene promoter regions[75,79].

1.6.5 BNIP3 transcriptional regulation by other factors

While hypoxia and HIF1 are best known to upregulate *BNIP3* expression, several other transcription factors that affect BNIP3 levels have also been identified. These include the energy stress regulator forkhead box O3a (FOX03a), signal transducer and activator of transcription 3 (STAT3), and cell division regulators E2F1 and tumour protein 53 (TP53)[30,80–84]. Transcription factors NFκB and E2F4 both participate in silencing of BNIP3 expression[30,84]. Several of these transcription factors, including HIF1, are regulated by reactive oxygen species (ROS).

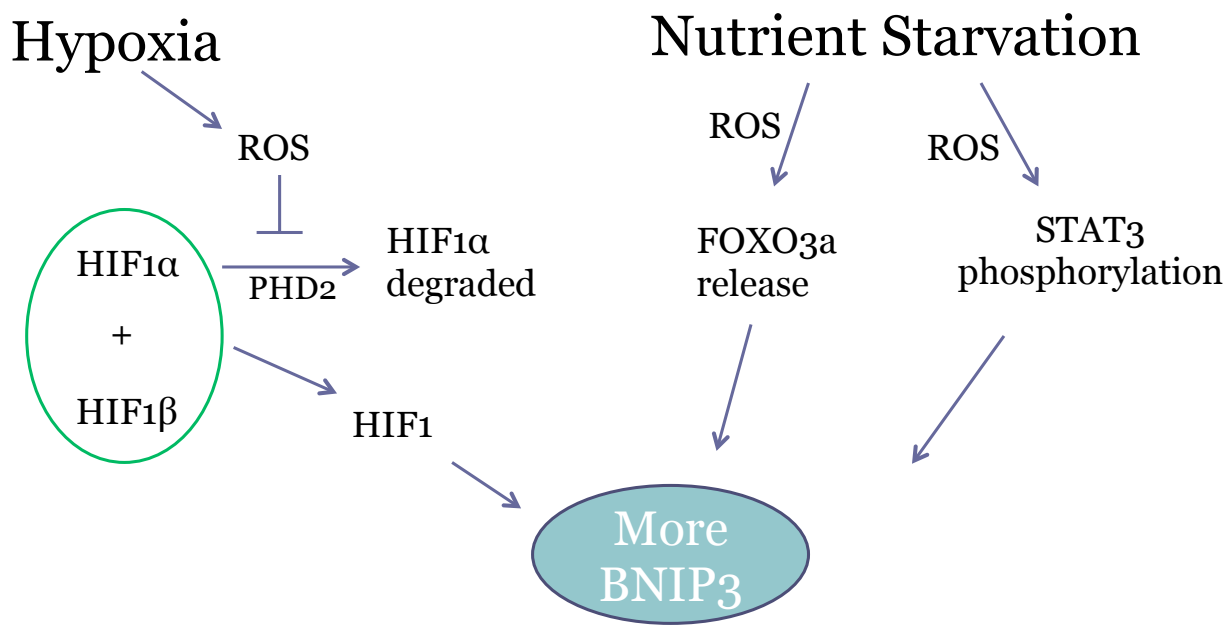

Figure 6: Transcriptional upregulation of *BNIP3* is mediated by reactive oxygen species (ROS). Degradation of HIF1α by the activity of prolyl hydroxylase 2 (PHD2) is inhibited during hypoxia, allowing formation of HIF1 and subsequent upregulation of *BNIP3*. Mounting evidence suggests that ROS participate in this process. Similarly, reactive oxygen species have been established as regulators of other transcription factors that upregulate *BNIP3,* such as FOXO3a and STAT3.

1.7 Oxidative Stress

Reactive oxygen species are a class of small, unstable, oxygen-containing molecules that include but are not limited to: hydrogen peroxide (H_2O_2), superoxide (O_2-), the hydroxyl radical (•OH), singlet oxygen (O•), and ozone (O_3)[85–87]. Oxidative stress occurs when the level of ROS in a cell exceeds the cell's capacity to prevent or repair the damage they cause[86]. The excessive ROS may be inappropriately localized at subcellular locations, be inappropriately present at the wrong time or for too long a period, or be the wrong type of ROS. However, ROS are required for a variety of cellular activities[86,87]. This section will describe endogenous sources of ROS, antioxidant systems, and ROS functions.

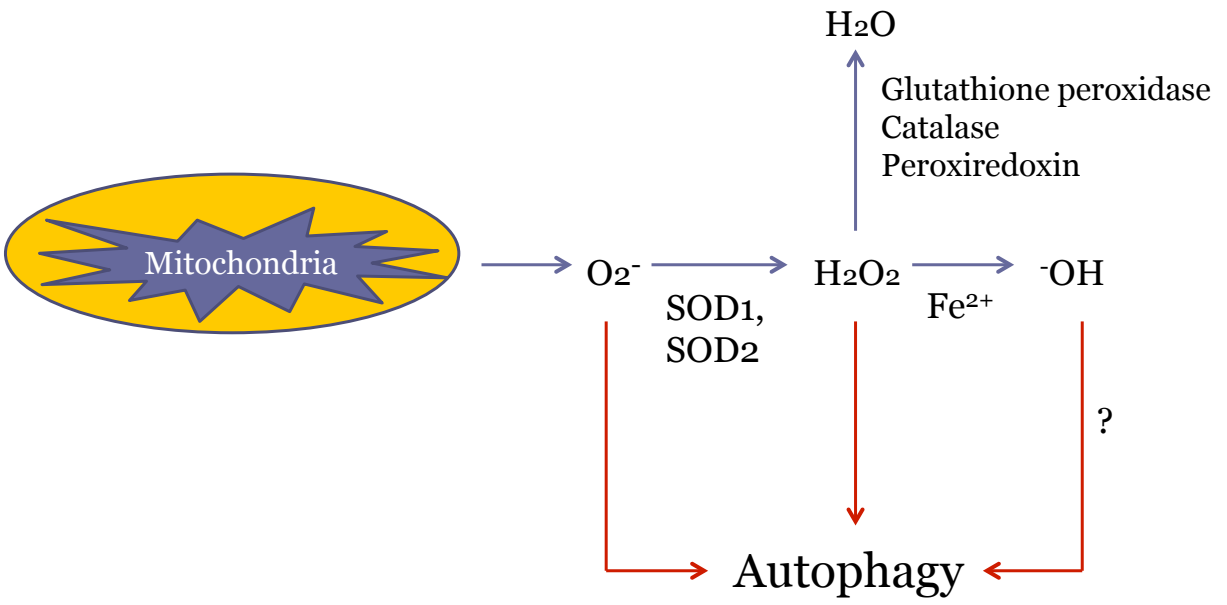

Figure 7: Reactive oxygen species produced by mitochondria are converted to other species or water through a series of reactions. Mitochondria are the primary source of reactive oxygen species in most cells. Superoxide (O_2^-) is rapidly converted to hydrogen peroxide (H_2O_2) by superoxide dismutases (SOD1 and SOD2). Hydrogen peroxide can then be converted to harmless water (H_2O) by various enzymes or to the very damaging hydroxyl radical (^-OH) in the presence of iron. Superoxide and hydrogen peroxide are known to induce autophagy. It is unknown whether the hydroxyl radical induces autophagy.

1.7.1 Endogenous sources of reactive oxygen species

Mitochondrial oxidative phosphorylation is the primary source of ROS in most cells, with production observed from complexes I and III of the electron transport chain (ETC), and to a lesser extent from complex II[85,88]. As electrons pass through the ETC, some interactions with proteins in the ETC lead to partial reduction of oxygen to form superoxide or hydrogen peroxide. Other sources of cellular superoxide include NADPH oxidases (NOX), xanthine oxidase, and a variety of other enzymes that participate in oxidation reactions[85,86,89,90]. Hydroxyl radicals are produced mainly by reaction of hydrogen peroxide with iron Fe^{2+} ions in a Fenton reaction[90].

1.7.2 Antioxidant systems

Maintenance of cellular homeostasis requires a mechanism for preventing or reducing excessive ROS production. Numerous enzymes are present in cells for the purpose of converting ROS into less reactive substances. These include but are not limited to: superoxide dismutases (SOD), which rapidly convert the highly reactive superoxide to the less reactive hydrogen peroxide; and catalases, glutathione peroxidases, thioredoxins and peroxiredoxins, which convert hydrogen peroxide to water[86,88,90,91]. These function in different subcellular locations. Aside from enzymatic catabolism of ROS, other mechanisms of removing ROS involve non-enzymatic catabolic reactions with small molecules such as ascorbic acid and a number of α-ketoacids, which act as buffers by cycling between oxidized and reduced versions in reaction with ROS[86].

1.7.3 Functions of reactive oxygen species

ROS perform both positive and negative functions within cells. Because they are highly reactive, ROS can reversibly or irreversibly alter proteins, lipids and DNA[87,88,92]. Reversible alterations may function in signalling, while irreversible alterations require repair or replacement of damaged macromolecules. For example, oxidized DNA may be repaired by base excision or nucleotide excision repair pathways, while irreversibly oxidized proteins and lipids may undergo proteasomal or autophagic degradation[86]. High levels of ROS damage proteins of the mitochondrial ETC, leading to disruption of oxidative phosphorylation, which in turn causes even higher production of ROS[88]. Excessive damage can lead to cell death[53,90,93].

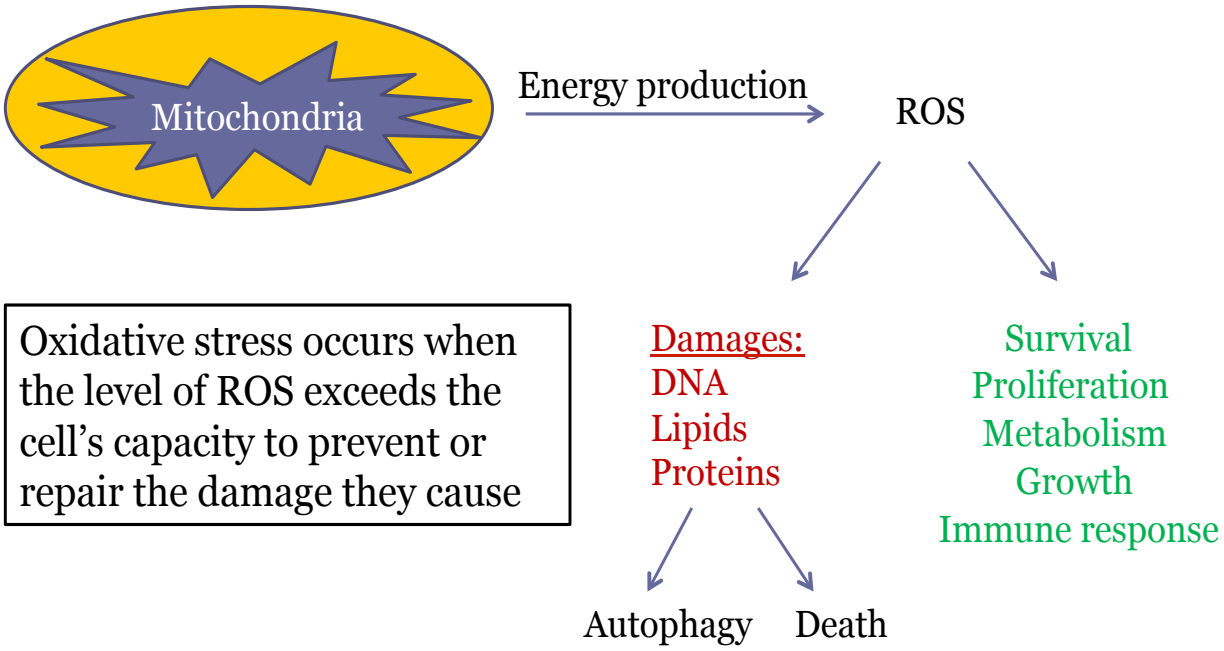

Figure 8: Reactive oxygen species (ROS) perform both positive and negative functions in cells. They are able to irreversibly damage DNA, lipids and proteins, but they may also act as signalling molecules that reversibly interact with proteins or DNA to perform important functions, or they may participate in immune response against invading bacteria. Excessive levels of ROS my cause cell death.

The type and extent of oxidative damage can depend on the type of ROS. Hydroxyl radicals are extremely and indiscriminately reactive and cause irreversible damage, but it is unknown how frequently hydroxyl radicals are produced in cells given that iron (needed for Fenton reactions) is sequestered in cells[87,88,90]. Superoxide is also highly reactive, but primarily inactivates iron-containing proteins via oxidation of sulphur residues, leading to iron loss[86,87]. Superoxide has also been shown to induce autophagy[91,94]. Hydrogen peroxide has a lower level of reactivity, giving it a longer half-life than superoxide, and is uncharged, making it capable of easily diffusing through membranes[88]. These features make hydrogen peroxide simultaneously more dangerous than superoxide and better able to act as a signalling molecule.

Redox signalling is essential for many cellular activities. Low levels of ROS can participate in localized signalling pathways, while higher levels of ROS can coordinate signalling throughout the cell[86]. ROS have been shown to regulate the activities of tyrosine and serine/threonine kinases such as epidermal growth factor receptor (EGFR), of tyrosine and serine/threonine phosphatases such as phosphatase and tensin homolog (PTEN), and of a variety of other important molecules such as heat shock proteins, histone deacetylases (HDACs), caspases, and zinc finger proteins[86]. Immune cells use a burst of hydrogen peroxide to damage invading bacteria, while transcription of many genes, such as those that encode antioxidant enzymes or growth factors, require transcription factor interaction with ROS or direct interaction of DNA with ROS[85,86]. Examples of transcription factors activated by ROS include FOXOs, STAT3, and HIF1[86,95–97]. Cell survival regulator NFκB may be either activated or inhibited by ROS[86]. As mentioned previously, these transcription factors are known to regulate BNIP3 expression, so ROS may also indirectly regulate BNIP3 expression.

In particular, ROS have been implicated in autophagy induction and cellular response to hypoxia. Hydrogen peroxide and superoxide have been shown to regulate autophagy in a number of ways, including by activating AMPK, leading to inhibition of mTOR and activation of autophagy, by upregulating expression of *BECN1,* and by oxidizing the autophagy protein responsible for conjugation of LC3 to autophagosomes[54,98–100]. Although the role ROS plays in hypoxia response is still an area of controversy, mounting evidence points to mitochondrial ROS as a participant in HIFα stabilization via inactivation of PHD2, the enzyme responsible for hydroxylation of HIFα[76,86,101–103]. Oxidation of cysteine residues in PHD2 leads to disulphide bond formation and subsequent inactivation by

homodimerization[101]. While it may seem counter-intuitive for reactive *oxygen* species to have a role in cellular response to low oxygen, the redox status of cytochrome c of the ETC changes in response to oxygen availability, making superoxide production more likely when oxygen levels are low[102]. However, PHD2 requires substrate oxygen to function, making it possible that hypoxia alone may be sufficient to reduce PHD2 activity.

1.7.4 Oxidative stress and cancer

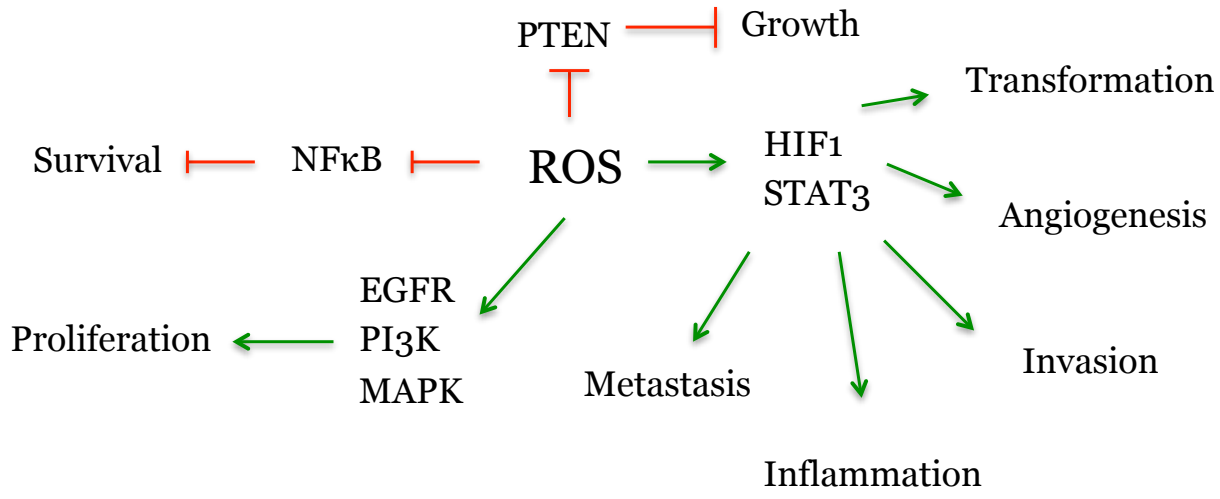

Figure 9: Reactive oxygen species (ROS) play many roles in tumorigenesis. Interaction with a variety of proteins promotes the spread and survival of tumours.

While ROS have many important functions in healthy cells, they also play roles in tumorigenesis. Cancer cells have increased localized ROS production due to increased metabolism, leading to increased DNA damage, chemoresistance and a variety of other effects[53,86,87,104]. By increasing the activity of growth factors such as EGFR, ROS increases proliferation of cancer cells, while inactivation of the tumour suppressor PTEN also stimulates unchecked growth[87]. ROS also affect cell survival through inhibition of NFκB, and proliferation through activation of PI3K and MAPK signalling pathways[87]. Activation of

other transcription factors such as HIF1 and STAT3 lead to angiogenesis, cell transformation, invasion, cancer-spreading inflammation, and metastasis[104,105]. Increased antioxidant activity in cancer cells help to maintain redox homeostasis and prevent death from oxidative stress, but excessive levels of ROS can still lead to cell death[53,87].

1.8 BNIP3 and Glioblastoma

Just as tumours are known to have high levels of ROS, they also are known to have high levels of HIF1 due to insufficiency of the vasculature to support the rapidly proliferating tissues[78,106]. This situation results in varying levels of hypoxia, which is very common in solid tumours. In response to hypoxia, HIF1 upregulates expression of genes involved in metabolic adaptation, inflammation, cell migration and metastasis, angiogenesis, cell survival and autophagy (*BNIP3*)[78,106]. However, high levels of BNIP3 induce cell death, enabling the protein to act as a tumour suppressor[80]. For this reason, many cancers silence *BNIP3* expression, including triple negative breast cancer (TNBC), pancreatic cancer, leukemia and lymphoma, colon cancer, and gastric cancer, leading to chemotherapy resistance and poorer patient outcomes[17,30,80,107–109]. This silencing can occur through gene deletion/copy number loss, histone deacetylation or gene promoter hyper-methylation. In contrast, over-expression of *BNIP3* in other cancers such as cancers of the breast (except TNBC), lung, endometrium, cervix, prostate, and brain, leading to more aggressive disease, chemotherapy resistance and poorer patient outcomes[17,68,69,110]. In cancers where *BNIP3* is over-expressed, BNIP3-induced cell death may be blocked by C-terminal phosphorylation[42] or by preferential expression of splice variant BNIP3, which acts as a dominant negative against the full length protein[15,33]. Nuclear localization of

BNIP3 has also been observed in cancers of the lung, breast, cervix, prostate, and in the majority of human gliomas[17,67,69].

The most common and most malignant form of adult glioma is glioblastoma (formerly glioblastoma multiforme), a grade IV astrocytoma with a median survival time of less than 15 months and a 5-year survival rate of 3-5%[111,112]. Patients are treated with surgery to remove as much of the tumour as possible, followed by radiation and chemotherapy, typically with temozolamide[111,113,114]. Despite this aggressive treatment combination, patient outcome is poor and most experience deadly recurrence of their disease[111,113]. Glioblastoma tumours rapidly outgrow their vasculature, leading to extensive regions of necrosis due to hypoxia[69,111]. BNIP3 expression is a poor prognosis marker for this disease, and plays a role in both cancer survival and treatment resistance[17,67–69]. It does this via BNIP3-mediated upregulation of pro-survival autophagy and transcriptional repression of pro-survival proteins, as described in other sections of this thesis.

1.9 Study Rationale, Hypothesis, and Objectives

While the role of BNIP3 in cellular response to hypoxia has been well studied, the role BNIP3 plays in cellular response to oxidative stress is still unknown. Current evidence suggests that reactive oxygen species may regulate BNIP3 expression and influence its activity, but a direct link has yet to be established. Both hypoxia and high levels of ROS are common in solid tumours such as glioblastoma, which also have high levels of BNIP3. The aim of this project is to determine whether ROS, in the absence of hypoxia, is able to regulate BNIP3 expression, localization and activity.

I hypothesize that oxidative stress increases expression of BNIP3 and causes mitochondrial localization, leading to increased cell death. This study will increase our knowledge of whether BNIP3 plays a role in cellular response to oxidative stress.

The specific objectives of this study are: (1) to determine the localization and expression levels of BNIP3 under oxidative stress; and (2) to determine the role of BNIP3 in oxidative stress-induced cell death

Chapter 2: Materials and Methods

2.1 Cell Culture

The human embryonic kidney cell line HEK293 was obtained from American Type Culture Collection (ATCC). The human glioblastoma cell line U87 was obtained from Dr. C. Hao, University of Alberta. Murine Embryonic Fibroblasts (MEFs) expressing BNIP3 (+/-) or lacking BNIP3 (-/-) were prepared by the University of Manitoba Genetic Modelling Centre. The BNIP3 -/- mice were obtained from Dr. Gerald Dorn (Washington University School of Medicine). The mouse model was generated using homologous recombination to replace *BNIP3* exons 2 and 3 with a neomycin cassette to create a truncated, null protein containing only the N-terminal region[115].

All cell lines were cultured in 100mm tissue culture dishes using HyClone Dulbecco's High Glucose Modified Eagles Medium (DMEM/High Glucose; GE Healthcare) supplemented with L-glutamine, L-glucose, and sodium pyruvate. HEK293 and U87 cells were cultured using 5% fetal bovine serum (FBS; Wisent Inc.), while MEFs were cultured using 10% FBS. To reduce oxidative stress, 0.11 mM beta-mercaptoethanol (BME; Gibco) was also added directly to MEF culture dishes at time of passage. This was omitted when culturing MEFs for experimentation. All cells were maintained in a humidified 37°C incubator with 5% CO_2 and split into new culture dishes once they reached 70-90% confluency.

Maintenance of cells

HEK293 cells are semi-adherent and were passaged by gently washing the cells from the plate with media before transferring an appropriate amount to a new culture dish for a 1/10 dilution of cells. When harvesting cells for experimentation, media was removed from the plate and 2 mL of 2.5% Trypsin-EDTA (Sigma) was used to lift cells from the plate and to reduce clumping. After incubating 1-2 minutes at room temperature, cells were pipetted gently to suspend and then mixed with 3 mL of complete media to quench the trypsin.

U87 and MEF cells are both adherent cell lines. U87 cells were passaged by removing media, adding 2 mL Trypsin-EDTA and incubating 1-2 minutes at 37°C. The cells were pipetted gently to suspend, mixed with 3mL of complete media and then transferred to a 15 mL conical tube with screw cap lid and centrifuged for 5 minutes at 290 x g. The supernatant was removed and the cell pellet was re-suspended in fresh media before transferring to new culture dishes for a 1/10 dilution of cells. MEFs were passaged by removing media and washing the cells with sterile 1X phosphate buffered saline pH 7.0 (PBS; Agilent Technologies). After incubating 2 minutes at 37°C in 3 mL Trypsin, the above procedure was followed as for U87 cells.

Cryopreservation of cells

Cells were preserved for future use by freezing cells once culture dishes reached 80-90% confluency. Cells were harvested by trypsinization as described above, and then pelleted by centrifugation at 290 x g for 5 minutes. The supernatant was removed and the cell pellet was resuspended in 1 mL of freezing media consisting of 500 µL DMEM/High

Glucose media, 300 µL FBS and 200 µL dimethyl sulfoxide (DMSO; Sigma). This was transferred to a cryovial (Sarstedt), which was then placed in a room temperature Nalgene container and frozen at -80°C. Once frozen, cryovials were relocated to nitrogen tanks for long-term storage.

Thawing frozen cells

Frozen cells were transported from nitrogen tanks on ice and then warmed briefly by hand. Thawed cells were then mixed with 4 mL of room temperature complete media, transferred to a 15 mL tube and then pelleted by centrifugation for 5 minutes at 290 x g. The supernatant was removed, cell pellets were resuspended in 10 mL of fresh media, and the solution was poured into a 100 mm culture dish. After 24 hours incubation at 37°C the media was changed and the cells were allowed to reach 80-90% confluency before passaging. Cells were passaged at least once before using for experimentation.

Hypoxia induction

Hypoxia was induced in cells by placing them in a hypoxic chamber (Fisher Scientific). Media was removed from the culture dish, which was then transferred to the chamber and cycled to remove oxygen. Once inside the chamber, cells were maintained using hypoxic media that had been in the chamber for at least three days to outgas all oxygen. Cells were incubated at 37°C with 5% CO_2, 10% H_2, and less than 1% O_2, with N_2 making up the remainder of the gases. Plates in hypoxia were harvested by trypsinization within the chamber and then transferred to 15 mL tubes before being centrifuged outside the chamber at 290 x g for 5 minutes.

2.2 Counting cells for experimentation

After harvesting by trypsinization as described above, cells were counted for experimentation using either manual counting with a haemocytometer or automatic counting with the TC20 Automated Cell Counter (Bio-Rad). For both methods, 20 µL of cells were mixed with 20 µL of 0.4% Trypan Blue (Sigma) and then 10 µL of this solution was pipetted into each side of the haemocytometer or automatic counter chip. When counting by haemocytometer, stained and unstained cells within 5 grids per side were counted manually with a fluorescent microscope. The values were averaged and multiplied by the dilution factor of 2 to find the number of cells x 10^4/mL. The number of dead cells was subtracted from the total number of cells to find the viability. I proceeded to set up the experiment if greater than 85% viability was obtained.

2.3 Oxidative stress induction

Oxidative stress was induced by treatment with hydrogen peroxide over a period of time as required by each assay. When treating cells, a 30% hydrogen peroxide solution (Sigma) was freshly diluted in double distilled water (ddH2O; Millipore) to a 100 mM stock concentration before further dilution in fresh media to the final concentration required by each assay.

2.4 Cell viability assays

Acridine Orange/Ethidium Bromide counting

HEK293 cells were seeded in 6-well dishes at a density of 3 x 10^5 cells/mL and treated the next day with 0-1000 µM H_2O_2 or 50µM etoposide (Sigma) for a cell death control. Cells were harvested 24 or 48 hours after treatment and pelleted by centrifugation

at 290 x g for 5 minutes. Cell pellets were resuspended in 200µL media with 2µL Acridine Orange/Ethidium Bromide solution (AO/EB) consisting of 100µg/mL of each in PBS, and placed on ice. After mixing vigorously, 10µL of cells were transferred to glass slides. Stained live (green) and dead (orange) cells were visualized under a fluorescence microscope and 300 cells were counted manually per slide.

Trypan blue exclusion assay

HEK293 and U87 cells were seeded in 12-well dishes at a density of 1 x 10^5 cells/mL. MEFs were seeded at a density of 0.25 x 10^5 cells/mL. Cells were treated next day in triplicate with 0-1000 µM H_2O_2 in complete media, and harvested after 24 or 48 hours. Media was transferred to labelled 1.5mL microtubes and then cells were harvested by trypsinization as described above. Cells were pipetted gently to disperse into solution, after which the trypsin was quenched with the reserved media and the mixture was transferred back into the labelled tubes. Tubes were centrifuged for 5 minutes at 290 x g, supernatant was removed, and then pellets were resuspended in 200µL 1x PBS and transferred to round bottom FACS tubes. To stain dead cells, 20 µL of 0.4% trypan blue solution was added to each tube. Samples were analyzed by flow cytometry using either the FL3 channel of a FACSCalibur (Becton Dickinson) with BD CellQuest Pro v.0.4 cf1b software, or the BL4 channel of a Novocyte (ESBE Scientific) with NovoExpress 1.2.4 software.

2.5 Western blotting

Cells were harvested with trypsin and pelleted as described above, reserving the media in an appropriately sized centrifuge tube. Supernatant was removed and pellets were resuspended in 1% NP-40 lysis buffer, consisting of 150 mM sodium chloride, 20 mM

Tris base (Sigma), 10% glycerol, 2 mM EDTA, and 1% NP-40 (Sigma). Before use, lysis buffer was mixed with cOmplete Protease Inhibitor tablet (Roche), 2 mM sodium orthovanadate (New England BioLabs) and 1 mM phenylmethanesulfonylfluoride (PMSF; Sigma). The cell suspension was alternately vortexed for 15 seconds and kept on ice 5 minutes for a total of 3 times before centrifugation at 4°C for 5 minutes at max speed to pellet debris. Supernatant was transferred to a 0.6 mL tube and the pellet was discarded.

Protein concentrations were determined by BCA assay in microplates using a Pierce BCA assay kit (Thermo Scientific) according to manufacturer instructions. Standards were tested in duplicate and samples were tested in triplicate with a 1:10 dilution in ddH_2O. Microplates were read using either a Spectramax 190 (Molecular Devices) with SOFTmax Pro v.3.1.2 software or an Epoch (BioTek Instruments) with Gen5 v2.09 software.

Ten percent poly-acrylamide gels were prepared for gel electrophoresis using a TGX Fast Cast Acrylamide kit (Bio-Rad) according to manufacturer instructions. Equal amounts of protein were prepared for western blot by mixing protein, ddH2O and 6x Loading buffer to a final concentration of 5% glycerol, 2% SDS, 1% beta mercaptoethanol (Sigma), 0.05% bromophenol blue (Sigma), and 20 mM Tris base. Samples were boiled at 98°C for 10 minutes, cooled briefly on ice and then centrifuged briefly to collect contents to bottom of tubes. Samples were then loaded into wells and separated by SDS-PAGE. Separated proteins were transferred to a 0.45 μM nitrocellulose membrane (Bio-Rad) via wet transfer for 1 hour at 24 V (1 amp). Membranes were blocked for 1 hour at room temperature in 5% non-fat milk dissolved in TBS-T (1X TBS, 0.1% Tween 20; Sigma) before incubation with primary antibody overnight in the cold room. See Table 1 for a list of primary antibodies and dilutions.

Membranes were washed next day in TBS-T and then incubated in secondary antibody for 1 hour at room temperature. See Table 2 for a list of secondary antibodies and dilutions. Membranes were again washed in TBS-T and then covered with Pierce ECL reagent (Thermo Scientific) before protein detection using either x-ray film or an ImageQuant LAS 500 imaging machine (GE Healthcare).

Table 2: Primary Antibodies

Antigen	**Host Species**	**Application (Dilution)**	**Source**	**Product #**
BNIP3	Rabbit pAb	WB (1:1000) IF (1:100)	Sigma	HPA00315
BNIP3 (ANa40)	Mouse mAb	WB (1:1000) IF (1:100)	Abcam	ab10433
β-Actin	Mouse mAb	WB (1:5000)	Sigma	A3853
α-Tubulin (11H10)	Rabbit mAb	WB (1:1000)	CST	2125S
HA-Tag (6E2)	Mouse mAb	WB (1:1000)	CST	2367S
His-Tag (27E8)	Mouse mAb	WB (1:1000)	CST	2366S

Table 3: Secondary Antibodies

Antigen	**Host Species**	**Conjugate (dilution)**	**Source**	**Product #**
Rabbit IgG	Goat	HRP (1:10,000)	Bio-Rad	170-6515
Mouse IgG	Goat	HRP (1:10,000) (1:20,000 for actin)	Bio-Rad	170-6516
Rabbit IgG	Goat	Biotinylated (1:200)	Vector Labs	BA-1000
Mouse IgG	Goat	Biotinylated (1:200)	Vector Labs	BA-9200
Biotin		Alexafluor 488 Streptavidin	Life Technologies	S11223

2.6 Immunofluorescence imaging of cells

Cells were seeded on glass coverslips in 24-well dishes at 50,000 cells per well and treated next day (U87) or after two days (HEK293) with 50-1000μM H_2O_2 for 24 hours. Cells were incubated with 400 nM MitoTracker Red CMXRos (Invitrogen) for 45 minutes and either fixed overnight at 4° with 200μL of 3.7% Formaldehyde in 1X PBS or for 15 minutes at room temperature with 2% paraformaldehyde in 1X PBS. Primary antibody was a 1:100 dilution of Rabbit anti-BNIP3 in 10% FBS/1X PBS/0.1% NP-40. Secondary antibody was a 1:200 dilution of Biotinylated Goat anti-Rabbit. Tertiary antibody was a 1:500 dilution of Streptavadin-conjugated Alexafluor 488. Incubation times were 1.5 hours each at room temperature, washing twice for 5 minutes in 1X PBS/ 0.1% NP-40 after each incubation period. Coverslips were placed cell-side down on slides with VECTASHIELD Antifade Mounting Medium with DAPI (Vector Labs) and visualized on an Olympus IX82 confocal microscope with FLUOVIEW 4.3 software.

2.7 Real time RT-PCR

HEK293 cells were seeded in 100 mm dishes at 1 x 10^6 cells per dish and allowed to grow for 2 days. They were treated on the 3rd day with 0-1000μM H_2O_2 or hypoxia for 5 hours and then harvested by gently washing the cells from the plate before transferring to a 15 mL tube and centrifuging for 5 minutes at 290 x g. Supernatant was removed and RNA was harvested using an RNeasy Mini kit (QIAGEN) according to manufacturer instructions. Genomic DNA was removed from harvested RNA samples using DNA-free DNA Removal kit (Invitrogen) according to manufacturer instructions. RNA concentration and purity were

determined using a NanoDrop 2000 spectrophotometer (Thermo Scientific), with a 260/280 ratio of 1.8 considered pure RNA.

cDNA was prepared from RNA using qScript cDNA SuperMix (Quanta Biosciences) according to manufacturer instructions. The cDNA was diluted 1:4 using ddH2O and PCR plates were set up using BNIP3, Actin and GAPDH PrimePCR assays (Bio-Rad) according to manufacturer instructions. No Reverse Transcriptase (NRT) and No Template (NT) controls were included in each run. A hypoxic sample was included as a positive control for BNIP3 expression. GAPDH mRNA increases under hypoxia.

2.8 ROS staining of cells

HEK293 and U87 cells were seeded in 6 well dishes at a density of 3 x 10^5 cells per well and allowed to grow 24 hours before treating with 1 mM hydrogen peroxide for 1 hour or 2 hours. Cells were harvested by trypsinization and centrifugation at 290 x g for 5 minutes. Working in the dark, cell pellets were resuspended in 200µL of 1X PBS with 3.2 µM of dihidroethidium (DHE; Sigma), 5 µM of CM-H2DCFDA (DCF; Life Technologies), or 5 µM of MitoSOX Red (Life Technologies). The cells were then incubated in the dark at 37°C for 15 minutes before transferring into round bottom FACS tubes and diluted with additional PBS. Samples were analyzed immediately along with unstained controls on a Novocyte flow cytometer using the BL1 channel for DCF, and the BL2 channel for DHE and MitoSOX Red.

2.9 TMRM staining of cells

HEK293 cells were seeded 3 x 10^5 per well in 6 well dishes and allowed to grow 24 hours before treating with hydrogen peroxide for 24 hours. Before the time point was

complete, some untreated cells were incubated with 10 μM FCCP (Abcam) for 15 minutes at 37°C as a positive control, after which all samples were incubated with 200 nM TMRM (Life Technologies) for 20 minutes at 37°C. Cells were then harvested in the dark, following usual procedures. Cell pellets were resuspended with 1X PBS and then transferred to FACS tubes. Samples were analyzed immediately along with unstained controls on a Novocyte flow cytometer using the BL2 channel.

2.10 Plasmid isolation

LB broth was prepared by combining 25 grams of LB broth powder (DIFCO) per litre of ddH2O and autoclaving to dissolve. For bacterial selection purposes, 1 μL of carbenicillin or kanamycin antibiotic (ThermoFisher) was used per mL of LB broth. Bacterial culture flasks containing LB broth were inoculated with DH5alpha competent bacteria (ThermoFisher) containing HA-tagged BNIP3 WT plasmid resistant to carbenicillin, or His-tagged BNIP3 ΔTM PTET vector resistant to kanamycin, originally prepared by previous members of the Gibson lab. The BNIP3 ΔTM plasmid has a deletion of amino acids 164-184, which is the entire transmembrane domain. The plasmids were incubated overnight in a 37°C shaker and were harvested next day using a Plasmid Maxi kit (QIAGEN) according to manufacturer instructions. Plasmid concentrations were determined using a NanoDrop 2000.

2.11 BNIP3 transient over-expression

HEK293 cells were seeded in 6 well dishes at a density of 5 x 10^5 cells per well and transfected at 60-70% confluency using Lipofectamine 2000 (Invitrogen). For the transfection, 1 μg each of pcDNA3.1 empty vector (Invitrogen), ΔTM BNIP3 or WT BNIP3

plasmid DNA was diluted in 100 µL Opti-MEM (Gibco) and combined drop-wise with 12 µL of Lipofectamine 2000 diluted in 30 µL Opti-MEM. After incubating at room temperature for 30 minutes, the transfection mixtures were further diluted in 1.2 mL Opti-MEM before using this mixture to replace media in the wells. Cells were incubated at 37°C in the transfection mixture for 4 hours before replacing with complete media. Cells were either harvested next day for western blot to confirm successful transfection or treated with hydrogen peroxide for 24 hours before harvesting for cell death assay.

2.12 BNIP3 knockdown using siRNA

HEK293 cells were seeded in 6 well dishes at a density of 5 x 10^5 cells per well and transfected at 60-70% confluency using Lipofectamine 2000. For the transfection, 200 pmol of BNIP3 siRNA was diluted in 250 µL Opti-MEM and combined drop-wise with 5 µL of Lipofectamine 2000 diluted in 250 µL Opti-MEM. After incubating at room temperature for 30 minutes, the transfection mixtures were further diluted in 2 mL Opti-MEM before using this mixture to replace media in the wells. Cells were incubated at 37°C in the transfection mixture for 4 hours before replacing with complete media. Cells were either harvested after two days for western blot to confirm successful knockdown or treated next day with hydrogen peroxide for 24 hours before harvesting for cell death assay.

2.13 Quantification and Statistical analysis

Quantification of western blots and immunofluorescent images was conducted using ImageJ software[116]. For western blot quantification, mean grey values were obtained for each band of interest and for background regions without bands, and then background values were subtracted and a ratio of the relative values was calculated for each band. To

obtain mean grey values for BNIP3 fluorescence, background fluorescence was first subtracted from each image and then a region of interest was drawn around each cell to measure. The JaCoP plugin of ImageJ was used to quantify colocalization of BNIP3 and mitochondria by measuring Pearson's correlation coefficient and Manders' overlap coefficients for each cell of interest.

Graphs for Figures 6 and 7 were prepared using Microsoft Excel. Preparation of all other graphs and statistical analysis of all data were conducted using GraphPad Prism 7. Two-way ANOVA and Sidak's multiple comparison tests were performed on Figures 2C, 2F, 12B, 13B, 15A, 15C, 16B, and 17. One-way ANOVA and Tukey's multiple comparison tests were performed on all other graphs that were analyzed. To avoid pseudoreplication of results, statistical analysis was only conducted on experiments that were performed more than twice (N=3 or greater), such that Figures 3, 4, and 15B were not analyzed.

A large "N" was used to signify the number of times an experiment was independently performed, while a small "n" was used to signify the number of technical replicates for each experiment. Statistical significance was noted in graphs as *p-value < 0.05, **p-value < 0.01, ***p-value < 0.001, ****p-value < 0.0001, or NS (not significant).

Chapter 3: Results

To determine the sensitivity of HEK293 cells to oxidative stress induced cell death following hydrogen peroxide treatment, I treated HEK293 cells with a range of hydrogen peroxide concentrations for 24 hours and then measured total cell death manually using acridine orange/ethidium bromide (AO/EtBr) staining. The amount of cell death with treatment increased in a range from about 170% (10 µM and 50 µM treatments) to 260% (1 mM treatment) compared to untreated cells (Figure 10A). The increase in cell death over time was then determined over a time course with 200 µM hydrogen peroxide treatment for 4-48 hours and was measured by AO/EtBr counts. Cell death increased by about 230% over time, in a time dependent manner, compared to untreated cells (Figure 10B).

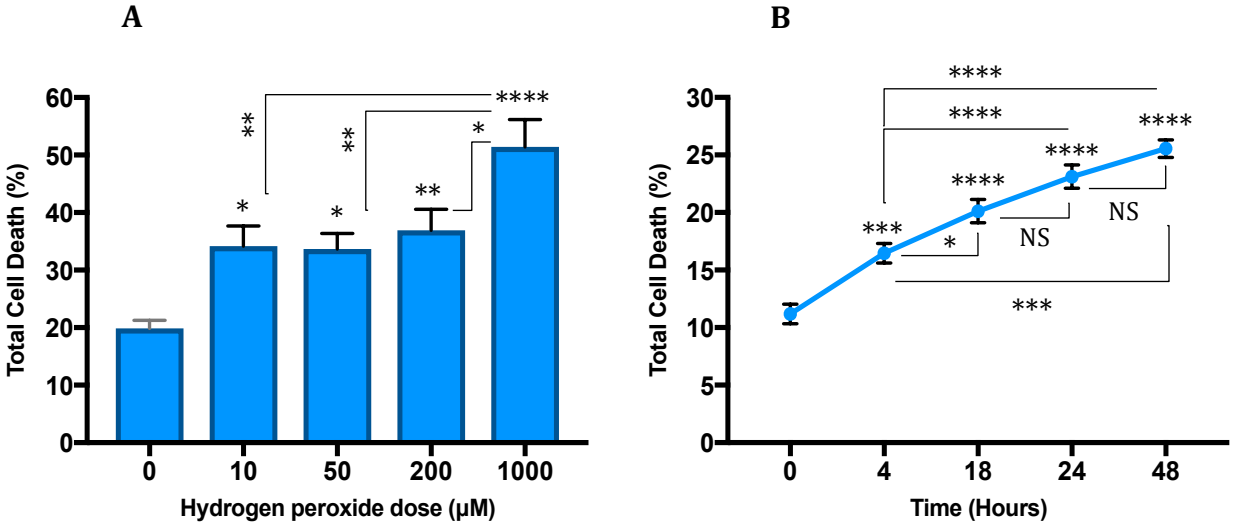

Figure 10: Total cell death increases with hydrogen peroxide treatment and time. (A) HEK293 cells were treated with 0-1000 µM hydrogen peroxide over 24 hours before staining with Acridine orange/Ethidium bromide and counting live/dead cells manually on a fluorescent microscope. N=5, n=1, with two counts per sample. (B) HEK293 cells were treated with 200 µM hydrogen peroxide over 48 hours and analyzed by Acridine orange/Ethidium bromide counting. N=4, n=2, with two counts (repeats) per sample. Bars represent standard error of the means. Except where noted with lines, significance stars are against the untreated control.

To complement the Acridine orange studies, I then proceeded to take additional cell death measurements using flow cytometry, this time treating both HEK293 cells and U87 cells with hydrogen peroxide for 24 and 48 hours and then staining with trypan blue, a fluorescent dye that permeates dead cells but not live cells. Flow cytometric analysis of cell death in HEK293 cells showed a dose-dependent response to hydrogen peroxide that was similar for both time points (Figure 10 A-C). Cell death in U87 cells was higher and more obviously dose-dependent after 48 hours treatment than after only 24 hours (Figure 10 D-F). The highest dose of hydrogen peroxide (1000 μM**)** lead to cell death in most of the populations of both cell lines, with averages of 75% and 86% death in U87 cells (at 24 and 48 hours respectively) and averages of 81% and 94% death in HEK293 cells (at 24 and 48 hours respectively). The second highest dose of hydrogen peroxide (800 μM) lead to average death percentages of 40% (24 hours) and 45% (48 hours) in HEK293 cells, and of 20% (24 hours) and 36% (48 hours) in U87 cells. Overall, these results suggest that oxidative stress affects cell populations in both a dose and a time-dependent manner.

To confirm that hydrogen peroxide was entering cells and causing increased levels of internal reactive oxygen species, I treated HEK293 cells with 1 mM hydrogen peroxide for 2 hours and then stained for internal hydrogen peroxide using CM-H2DCFDA, for superoxide using DHE, and for mitochondrial superoxide using MitoSox Red (Figure 12). These dyes only produce fluorescence once metabolized in the presence of ROS. Cellular levels of both hydrogen peroxide and superoxide increased following hydrogen peroxide treatment, with an average 4.8-fold increase in internal hydrogen peroxide levels, an average 1.7-fold increase in general superoxide levels, and an average 3.9-fold increase in mitochondrial superoxide levels.

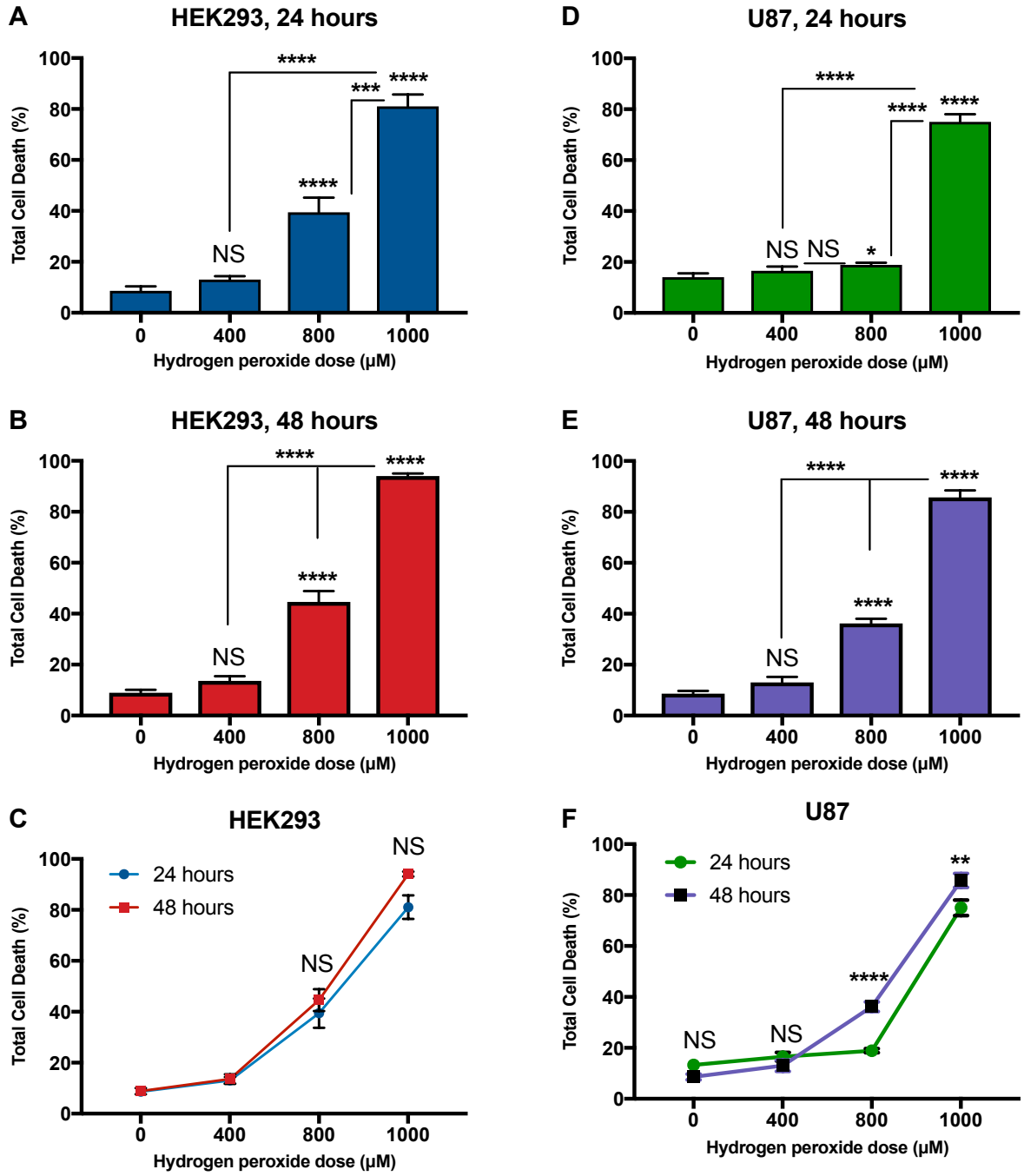

Figure 11: Total cell death increases with hydrogen peroxide treatment in HEK293 and U87 cells in a dose-dependent manner. (A) Total cell death in HEK293 cells treated with hydrogen peroxide for 24 hours, as analyzed by flow cytometry with trypan blue. (B) Total cell death in HEK293 cells treated for 48 hours. (C) Comparison of total cell death at 24 and 48 hours in HEK293 cells. (D) Total cell death in U87 cells treated for 24 hours. (E) Total cell death in U87 cells treated for 48 hours. (F) Comparison of total cell death at 24 and 48 hours in U87 cells. N=3, n=3. Bars represent standard error of the means.

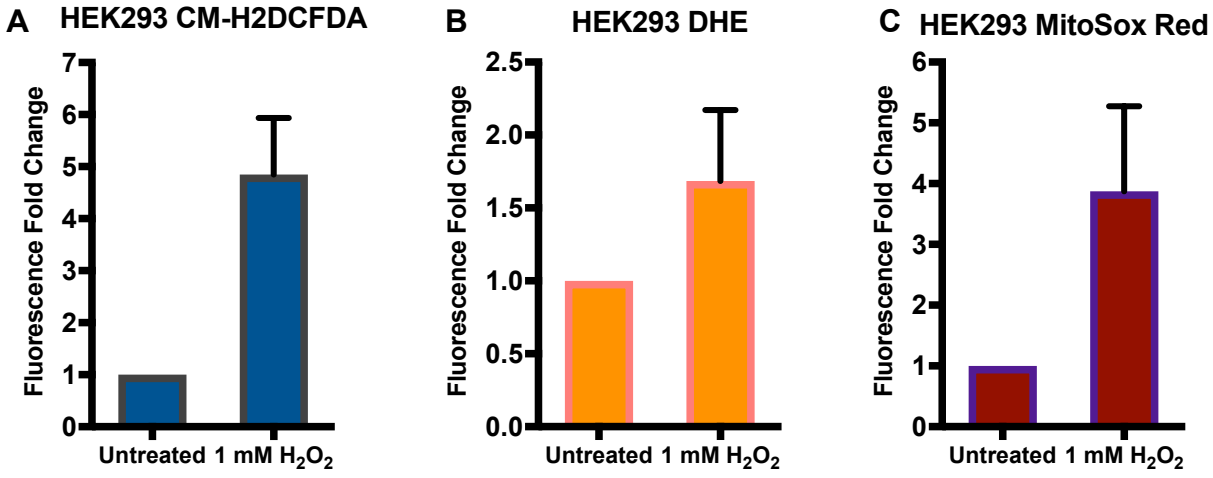

Figure 12: Oxidative stress increases internal reactive oxygen species in HEK293 cells. HEK293 cells were treated with hydrogen peroxide for 2 hours and then analyzed for relative ROS levels by flow cytometry. (A) Fold change in percent fluorescence with CM-H2DCFDA staining for cellular hydrogen peroxide. N=2, n=3. (B) Fold change in percent fluorescence with DHE staining for cellular superoxide. N=2, n=3. (C) Fold change in percent fluorescence with MitoSox Red staining for mitochondrial superoxide. N=1, n=3. Bars represent standard deviation.

I stained U87 cells with CM-DCFDA and MitoSox Red treated U87 cells and treated with hydrogen peroxide for one hour (Figure 13). Cellular levels of both hydrogen peroxide and mitochondrial superoxide increased following hydrogen peroxide treatment, with an average 20-fold increase in hydrogen peroxide levels and an average 1.4-fold increase in mitochondrial superoxide levels. Although the U87 cells were treated for less than the HEK293 cells, the increase in cellular hydrogen peroxide levels seen in U87 cells was considerably higher than the increase seen in HEK293 cells (20-fold vs. 4.8-fold). Mitochondrial superoxide levels increased less in U87 cells than in HEK293 cells (1.4-fold vs. 3.9-fold) but this can be explained by the shorter treatment time.

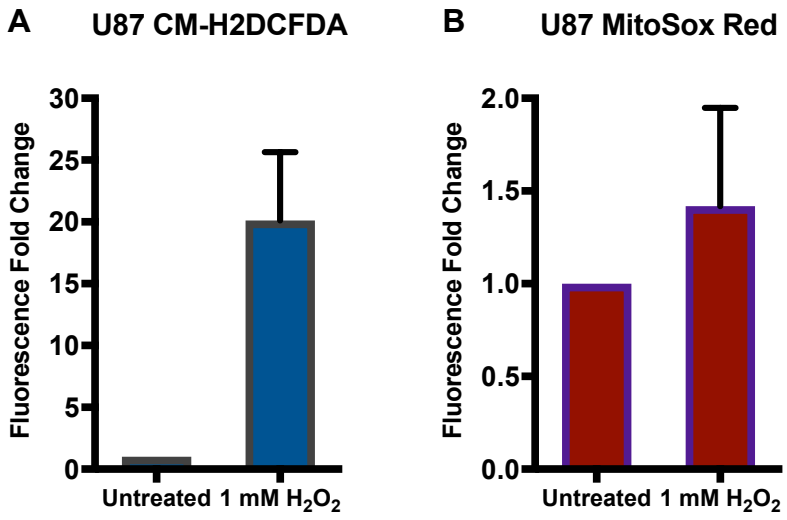

Figure 13: Oxidative stress increases internal reactive oxygen species in U87 cells. U87 cells were treated with hydrogen peroxide for 1 hour and analyzed for relative ROS levels by flow cytometry. (A) Fold change in percent fluorescence with CM-H2DCFDA staining for cellular hydrogen peroxide. N=1, n=3. (B) Fold change in percent fluorescence with MitoSox Red staining for mitochondrial superoxide. N=1, n=3. Bars represent standard deviation.

To determine whether oxidative stress was affecting mitochondrial membrane potential, I treated HEK293 cells with two concentrations of hydrogen peroxide for 24 hours and then stained with TMRM, a cationic dye that is readily sequestered in negatively charged (polarized) mitochondria but not in more positively charged (depolarized) mitochondria (Figure 14). For a positive control I treated cells for 15 minutes with FCCP, an electron transport chain uncoupler that causes mitochondrial membrane depolarization by increasing proton entry to make the internal environment more positively charged[117]. Untreated cells had an average median TMRM fluorescence intensity of 66,900, which dropped to an average of 12,900 with FCCP treatment. While treatment with the lower concentration of hydrogen peroxide, 400 μM, did not produce a statistically significant

change in median TMRM fluorescence intensity, the average intensity decreased to 59,800. Meanwhile, the higher concentration of hydrogen peroxide, 800 µM, significantly decreased median TMRM intensity to 19,600.

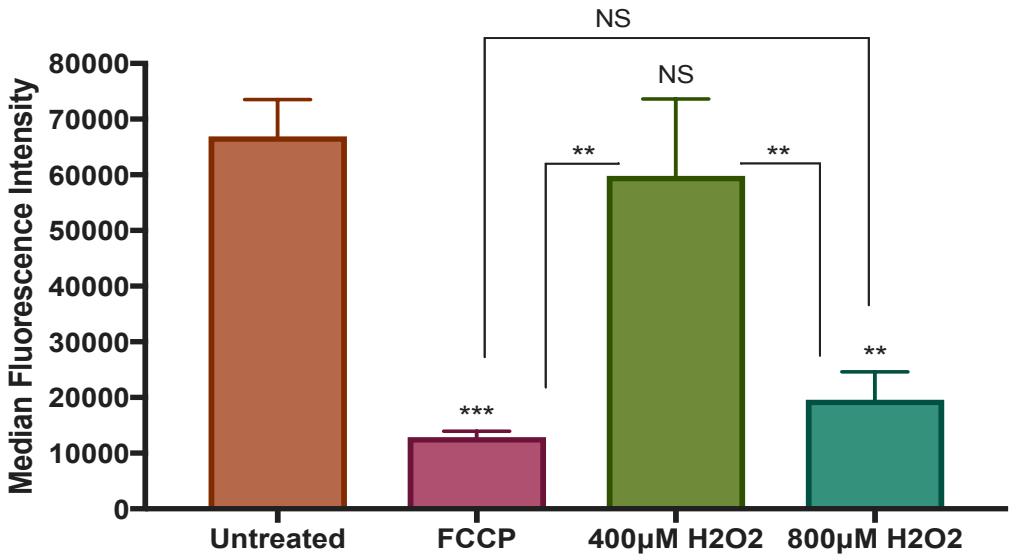

Figure 14: Oxidative stress reduces mitochondrial membrane potential. HEK293 cells were treated with hydrogen peroxide for 24 hours or FCCP for 15 minutes to disrupt mitochondrial membrane potential. Median fluorescence intensity of TMRM dye was measured by flow cytometry. N=3, n=3. Bars represent standard error. Except where noted with lines, significance level is against untreated. NS = Not Significant.

Next I wanted to establish whether BNIP3 protein levels increased with hydrogen peroxide treatment. I treated HEK293 and U87 cells with either hypoxia (as a positive control) or a range of hydrogen peroxide concentrations for 24 hours and then lysed cells and western blotted for BNIP3 protein levels. β-actin protein levels were also probed for as a loading control. In HEK293 cells, hydrogen peroxide treatment increased BNIP3 protein dimer levels progressively by averages of 2.7-fold (10 µM hydrogen peroxide) to 3.1-fold (1 mM hydrogen peroxide) compared to the untreated control (Figure 15). By comparison, hypoxia increased BNIP3 dimer levels by an average of 9.1-fold. BNIP3 protein levels for

cells treated with lower concentrations of hydrogen peroxide varied considerably from blot to blot, and actin levels for the hypoxia sample on each blot were consistently lower, presumably because very small volumes were needed to obtain the same amount of protein for this sample. This may have affected loading accuracy. Bands for the BNIP3 monomer were not visible on the HEK293 western blots except for in the hypoxia lane, so I was unable to assess whether BNIP3 monomer levels changed in HEK293 cells with hydrogen peroxide treatment.

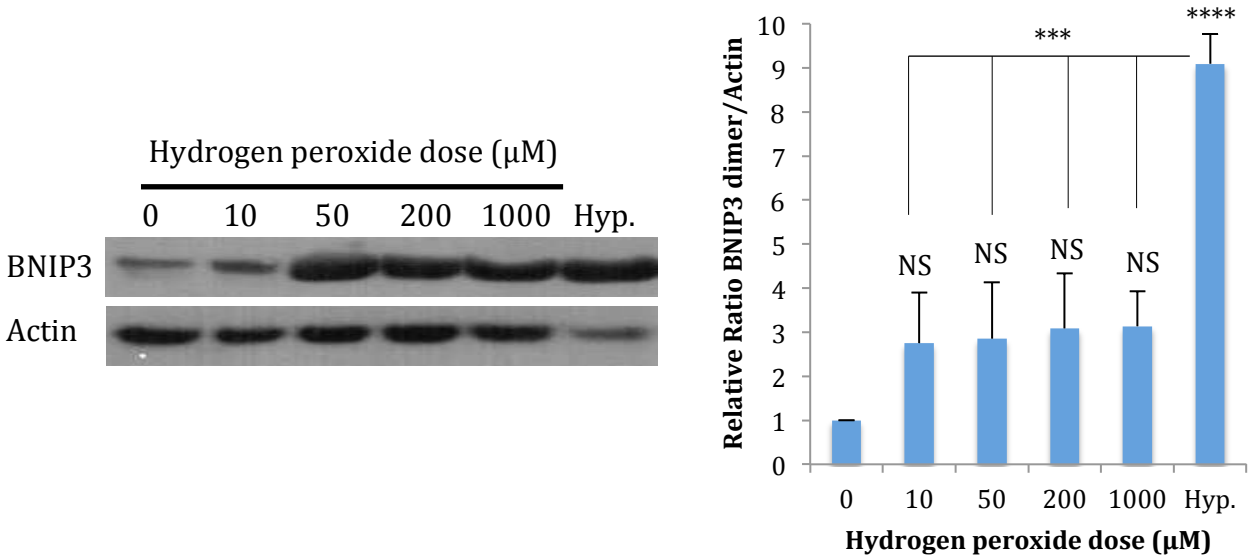

Figure 15: Oxidative stress increases BNIP3 protein levels in HEK293 cells. Cell lysates were harvested for western blot after treatment with hydrogen peroxide or hypoxia for 24 hours. Levels of the BNIP3 dimer (60 kDa) and β-Actin (42 kDa) were quantified using ImageJ software. N=3. Bars represent standard deviation. Except where noted with lines, significance is against untreated control. Lines show significance against hypoxic control only. Hyp. = Hypoxia

There was no increase of BNIP3 levels in U87 cells, as hydrogen peroxide treatment decreased BNIP3 protein dimer levels by averages of 0.81 for the 50 μM hydrogen peroxide treatment, 0.96 for the 200 μM hydrogen peroxide treatment, and 0.88 for the 1 mM

hydrogen peroxide treatment (Figure 16). Levels of the BNIP3 monomer also appeared to decrease, with 1 mM hydrogen peroxide treatment decreasing monomer levels by an average of 0.53. As a positive control, hypoxia increased BNIP3 dimer levels by at least 4.5-fold and increased monomer levels by at least 3.7-fold (data not shown). As with HEK293 cells, actin levels for the hypoxia sample were consistently lower, presumably due to smaller volumes loaded.

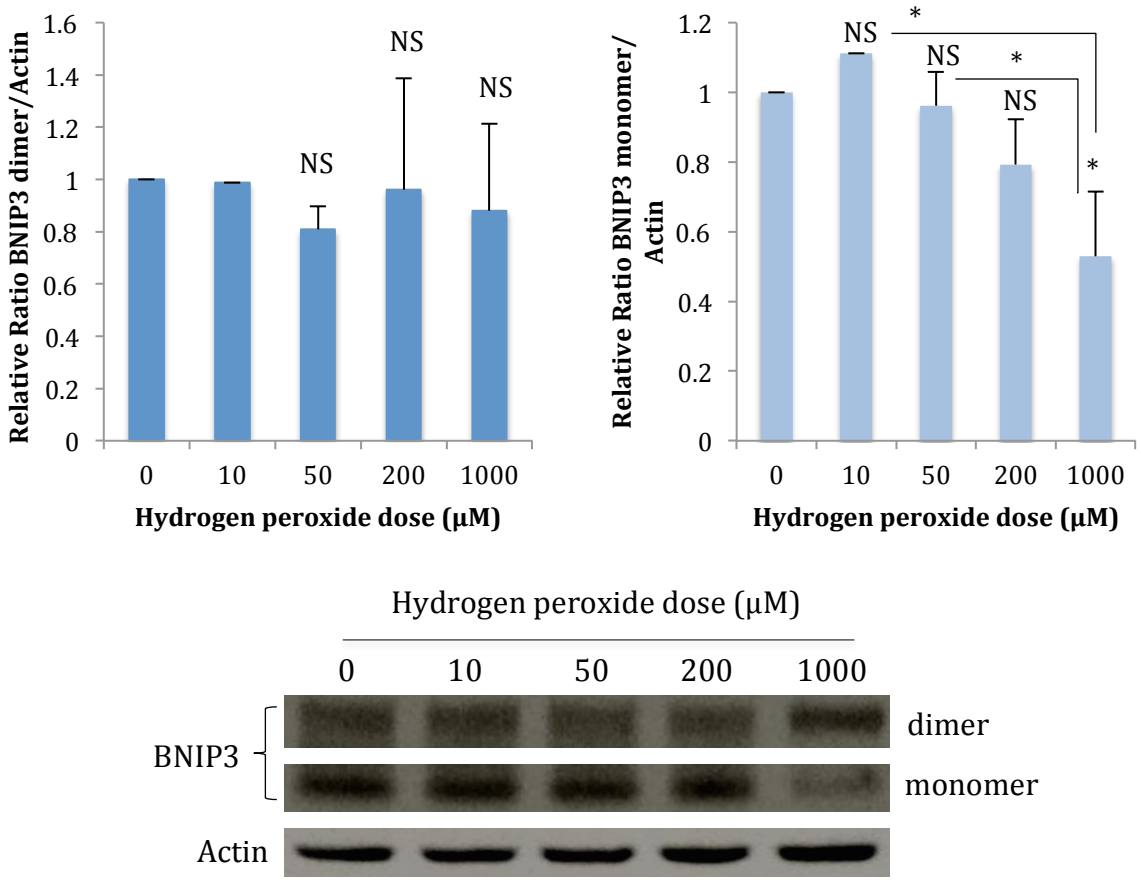

Figure 16: Oxidative stress does not increase BNIP3 protein levels in U87 cells. Cell lysates were harvested for western blot after treatment with hydrogen peroxide for 24 hours. Levels of the BNIP3 dimer (60 kDa), BNIP3 monomer (30 kDa) and β-Actin (42 kDa) were quantified using ImageJ software. N=3. Bars represent standard deviation. NS = not significant.

Analysis of *BNIP3* mRNA levels in HEK293 cells was conducted by quantitative RT-PCR after treatment with a range of hydrogen peroxide concentrations for 5 hours (Figure 17). Primers for *β-Actin* and *GAPDH* were used as standards, and treatment with hypoxia was used as a positive control. I found that this short exposure to oxidative stress gradually increased *BNIP3* mRNA levels in a dose-dependent manner, from a 1.15-fold increase with a 10 μM hydrogen peroxide treatment up to an average 1.4-fold increase with a 1 mM hydrogen peroxide treatment. In comparison, hypoxia dramatically increased *BNIP3* mRNA levels by an average of 25.8-fold relative to the untreated control (data not shown). This suggests that acute oxidative stress does not induce *BNIP3* gene expression as strongly as hypoxia does.

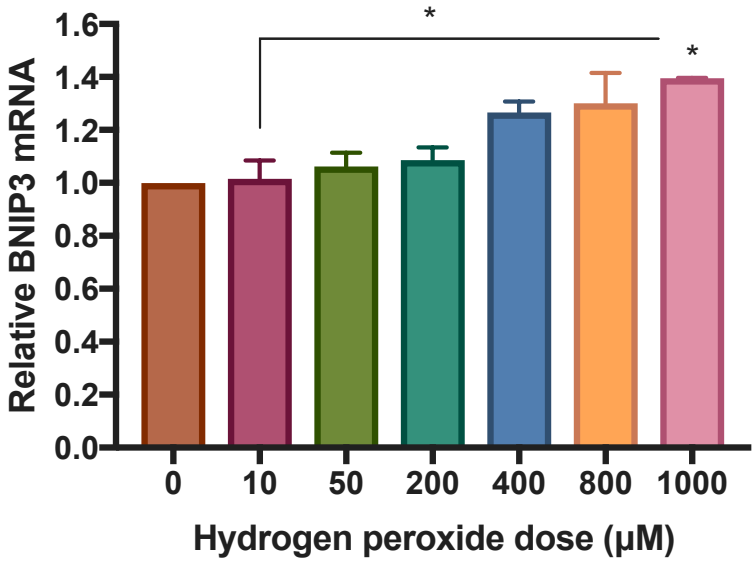

Figure 17: Oxidative stress increases *BNIP3* mRNA levels in HEK293 cells. BNIP3 mRNA levels after treatment with hydrogen peroxide, relative to untreated control. RNA was harvested from HEK293 cells following stimulation with hydrogen peroxide for 5 hours. Analysis of *BNIP3* mRNA levels was by qRT-PCR using primers for *BNIP3*, *β-Actin* and *GAPDH.* N=3, n=3. Bars represent standard error.

To determine whether BNIP3 localizes to mitochondria during oxidative stress, I seeded HEK293 and U87 cells on coverslips, treated with hydrogen peroxide for 24 hours and then performed immunofluorescent staining of BNIP3 and mitochondria. In HEK293 cells, oxidative stress appears to heighten both BNIP3 fluorescence and colocalization with mitochondria in a dose-dependent manner, as indicated by the increasing amount of yellow colour in the merged images with increasing doses of hydrogen peroxide (Figure 18). In U87 cells, BNIP3 was clearly localized to both the nucleus and cytosol of treated and untreated cells (Figure 19). In untreated U87 cells the mitochondrial fluorescence is noticeably tubular in appearance, which is suggestive of intact mitochondria, while in U87 cells treated with 800 μM hydrogen peroxide the mitochondrial fluorescence is punctate in appearance, which is suggestive of mitochondrial fission and fragmentation[118].

To confirm whether oxidative stress increases BNIP3 fluorescence intensity in HEK293 and U87 cells, I measured the mean grey value for BNIP3 fluorescence in the immunofluorescence images (Figure 20). I found that BNIP3 fluorescence increases in HEK293 cells in a dose-dependent manner, but changes as a bell curve in U87 cells, with fluorescence levels increasing with 200 μM hydrogen peroxide treatment and decreasing again to untreated levels with higher doses. This suggests that BNIP3 levels do not increase in a dose-dependent manner in U87 cells, which is consistent with western blot results.

To confirm whether oxidative stress increases BNIP3 colocalization with mitochondria in HEK293 and U87 cells, I measured both Pearson's and Manders' coefficients for immunofluorescent cells. Pearson's coefficient is a measure of the linear relationship or correlation between the positions of two fluorescent signals, with a value

between -1 (mutual exclusion) and +1 (complete colocalization)[119]. Manders' coefficients are measures of the proportion of overlapping pixels in both fluorescent channels, with values between 0 (no overlap) and 1 (complete colocalization)[119]. For this study, the M1 value indicates the fraction of total BNIP3 fluorescence that overlaps with mitochondrial fluorescence, while the M2 value indicates the fraction of total mitochondrial fluorescence that overlaps with BNIP3 fluorescence.

For HEK293 cells, the Pearson's coefficient value increased with hydrogen peroxide treatment in a dose-dependent manner (from 0.34 for untreated to 0.51 for 1 mM H_2O_2 -treated cells), demonstrating that colocalization of BNIP3 with mitochondria also increases in a dose-dependent manner (**Figure 21**A). Values for the Manders' coefficients suggest a general increase in the fraction of BNIP3 fluorescence overlapping with mitochondria (from 0.48 for untreated to 0.85 for 1 mM H_2O_2 –treated cells), while the fraction of mitochondrial fluorescence overlapping with BNIP3 also seems to increase compared to untreated cells, but in a bell curve with the lowest fraction of overlap (0.29) seen in untreated cells and the highest fraction of overlap (0.8) occurring in 50 μM H_2O_2-treated cells (**Figure 21**B).

For U87 cells, the Pearson's coefficient value did not appreciably change with H_2O_2 treatment, as both treated and untreated cells showed a considerable amount of colocalization (**Figure 22**A). Values for the Manders' coefficients likewise showed there was no meaningful change to the fractions of overlapping fluorescence with hydrogen peroxide treatment (**Figure 22**B). The majority of mitochondrial fluorescence was colocalized with BNIP3 fluorescence across all conditions (from 0.77 for the 800 μM H_2O_2

condition to 0.88 for the 50 µM H_2O_2 condition), while a consistently lower proportion of BNIP3 fluorescence was colocalized with mitochondrial fluorescence (from 0.49 for the 50 µM H_2O_2 condition to 0.53 for the 800 µM H_2O_2 condition).

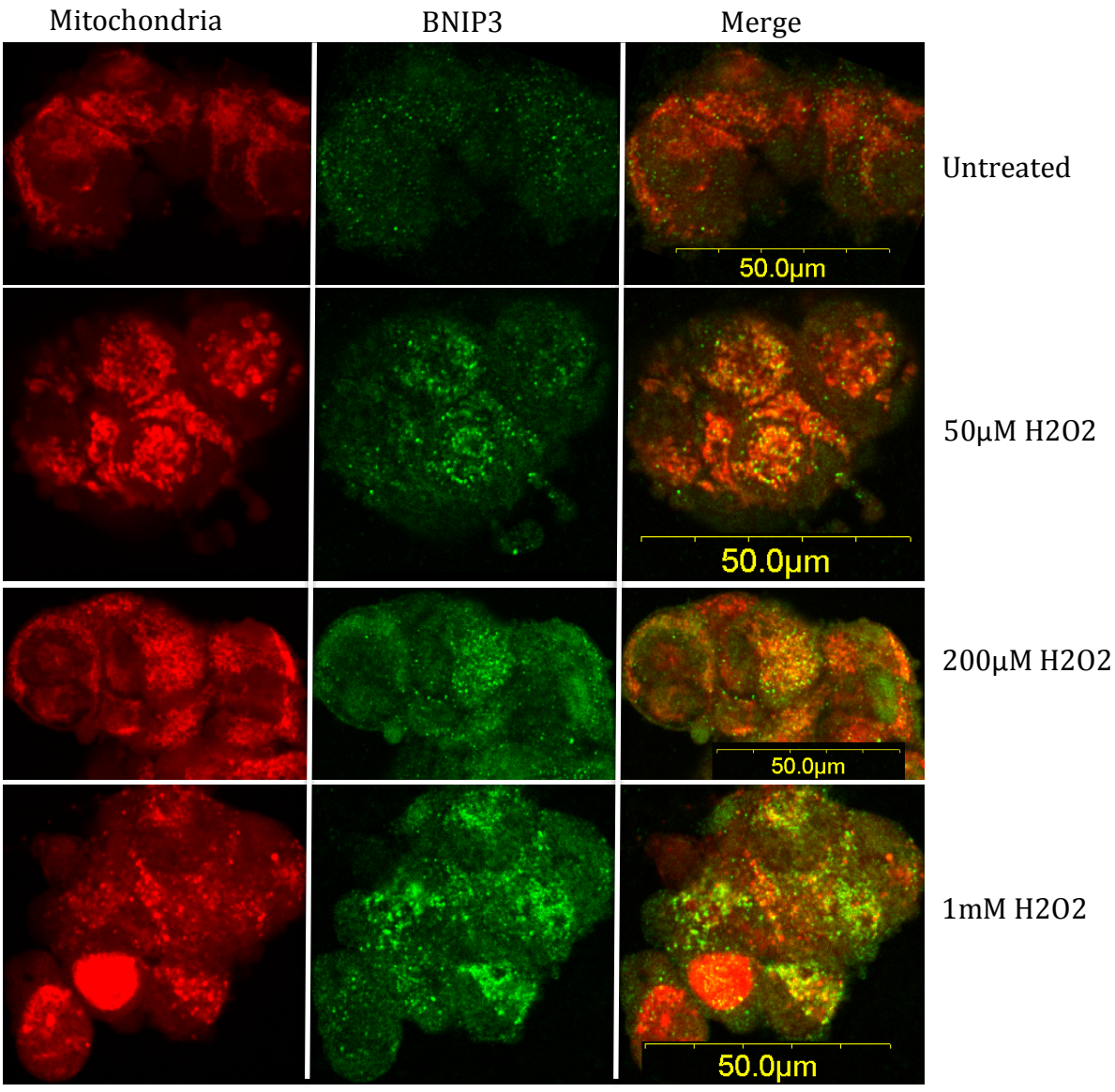

Figure 18: Oxidative stress increases localization of BNIP3 with mitochondria in HEK293 cells. Representative images of immunofluorescent staining of BNIP3 and mitochondria in HEK293 cells treated with hydrogen peroxide for 24 hours. Images were captured on a confocal microscope using line sequential scanning. Each image is of a cluster of cells.

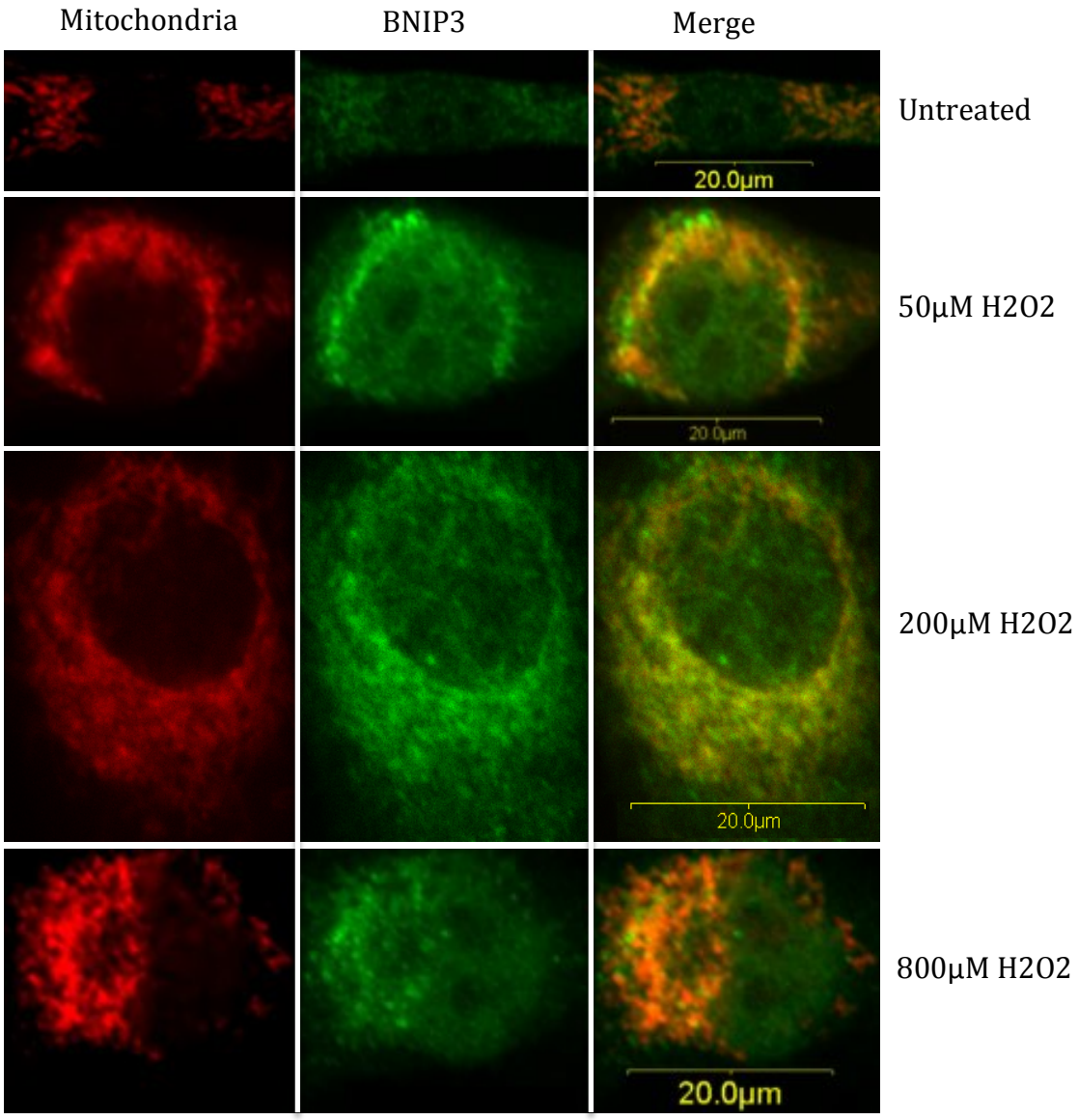

Figure 19: Oxidative stress increases localization of BNIP3 with mitochondria in U87 cells. Representative images of immunofluorescent staining of BNIP3 and mitochondria in HEK293 cells treated with hydrogen peroxide for 24 hours. Images were captured on a confocal microscope using line sequential scanning. Each image is of a single cell.

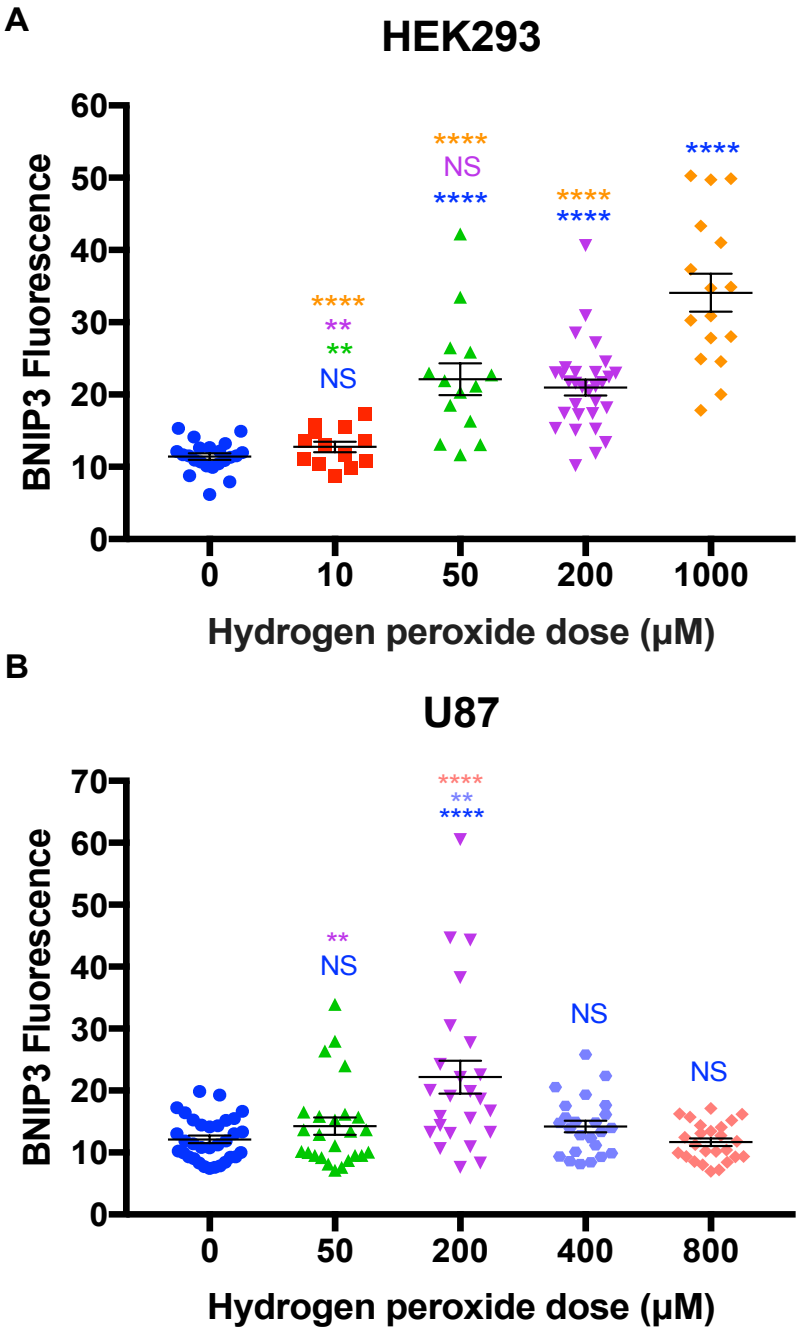

Figure 20: BNIP3 fluorescence increases in a HEK293 dose-dependent manner in HEK293 cells but not in U87 cells. Mean grey values for BNIP3 immunofluorescence in (A) HEK293 and (B) U87 cells treated with hydrogen peroxide for 24 hours. At least 14 HEK293 cells and at least 24 U87 cells were quantified per condition using ImageJ software. Bars are mean with standard error. Colour of significance stars corresponds to each comparison (e.g., blue stars indicates comparison with untreated condition)

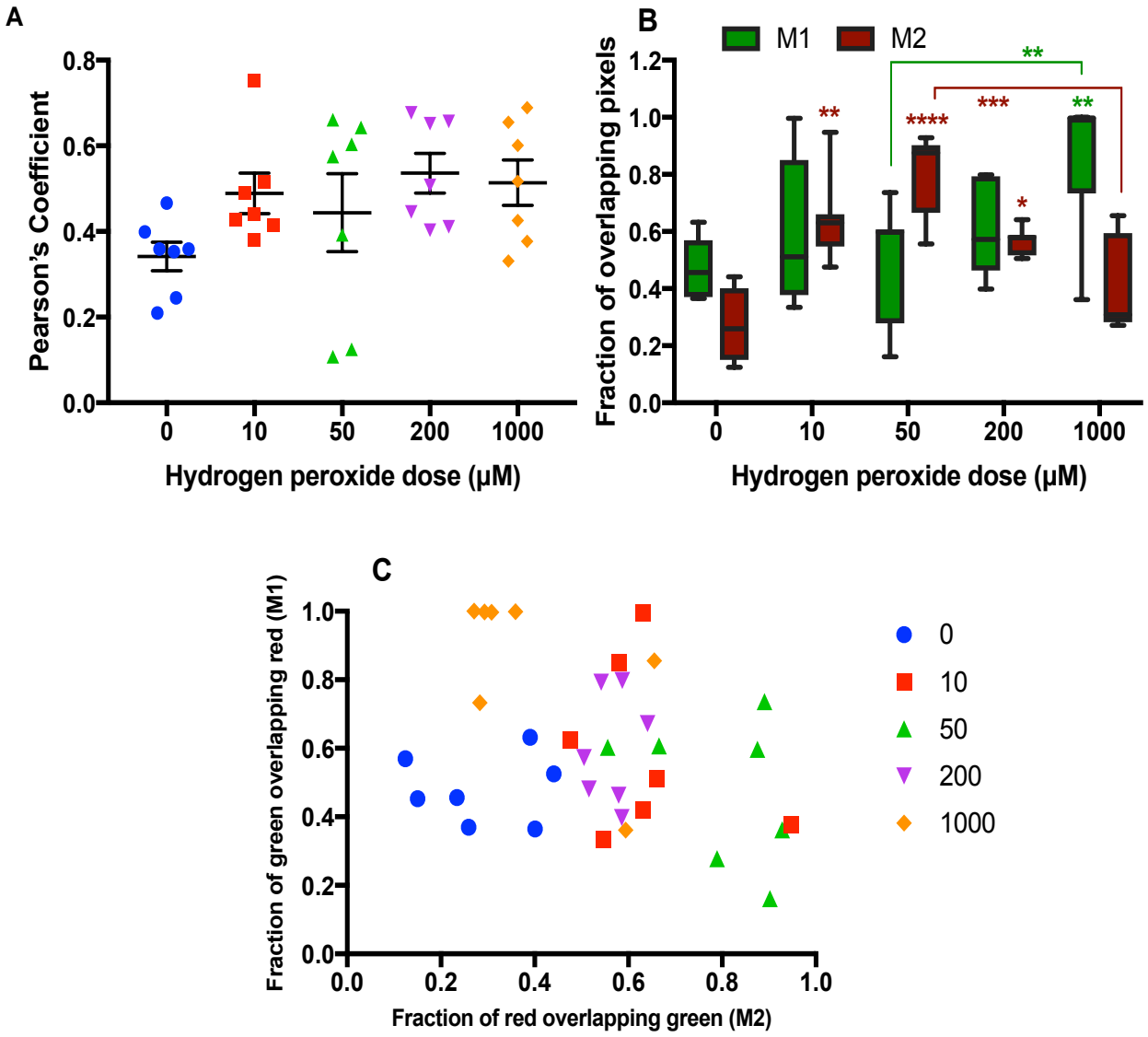

Figure 21: Colocalization analysis for immunofluorescent HEK293 cells. (A) Pearson's coefficient showing correlation between pixel locations for BNIP3 and mitochondria. There were no significant differences between means. (B) Bar graph of the Manders coefficients showing means of the fractions of overlapping BNIP3 (M1) and Mitochondria (M2) pixels. Except where noted with lines, significance stars are against untreated. (C) Manders coefficients showing fractions of overlapping green (BNIP3) and red (Mitochondria) pixels. Seven (7) cells were quantified per condition using ImageJ software.

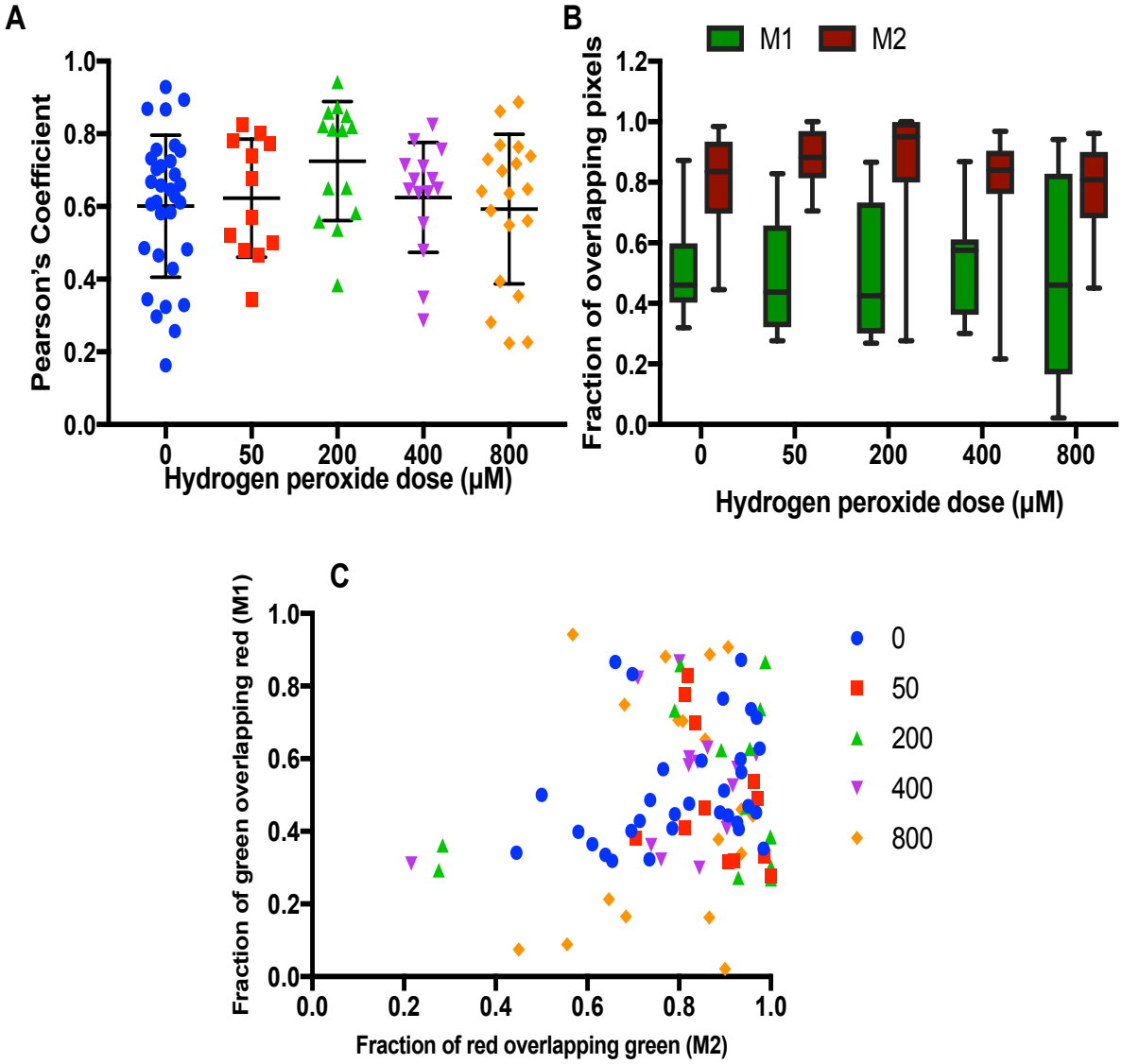

Figure 22: Colocalization analysis for immunofluorescent U87 cells. (A) Pearson's coefficient showing correlation between pixel locations for BNIP3 and mitochondria. (B) Bar graph of the Manders coefficients showing means of the fractions of overlapping BNIP3 (M1) and Mitochondria (M2) pixels. (C) Manders coefficients showing fractions of overlapping green (BNIP3) and red (Mitochondria) pixels for each cell. At least 12 cells were quantified per condition using ImageJ software. There were no significant differences between means.

I next transfected HEK293 cells with empty pcDNA3 vector, HA-tagged wild-type (WT) BNIP3 or His-tagged ΔTM BNIP3 over-expression vectors to explore the role BNIP3 was playing in oxidative stress-induced cell death. The ΔTM BNIP3 vector encodes a truncated version of BNIP3 that can act as a dominant negative against the full-length protein, so over-expression of this truncated protein would interfere with the activity of endogenous BNIP3. I confirmed over-expression of WT and ΔTM BNIP3 by collecting cell lysates 24 hours after transfection and western blotting for HA-tag, His-tag and BNIP3 (Figure 23). Ponceau stain was used to confirm loading (data not shown). Transfection efficiency was approximately 80% at 48 hours after transfection, based on co-transfection with GFP.

I treated the transfected cells for 24 hours with 200 μM hydrogen peroxide and measured cell death by staining cells with AO/EtBr and counting manually with a fluorescent microscope (Figure 24A). Average death in cells transfected with WT BNIP3 was markedly higher than in cells transfected with the control vector or ΔTM BNIP3, with a mean of 26.4% death for WT BNIP3 cells compared with means of 15.8% for control cells and 14.8% for ΔTM BNIP3 cells. Average death after hydrogen peroxide treatment was similar across conditions, with only a slight increase in death for control cells and ΔTM BNIP3 cells (20.6% and 18.6% respectively). Strangely, hydrogen peroxide treatment led to a decrease in average cell death for WT BNIP3 cells (22.3% with treatment vs. 26.4% without treatment).

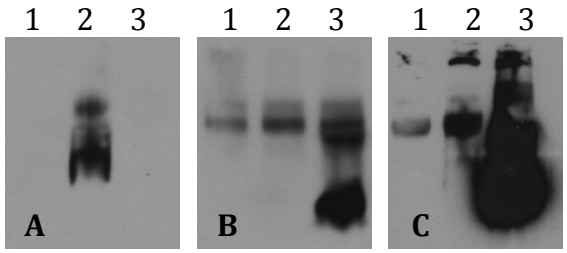

Lane 1: pcDNA3 vector
Lane 2: HA-tagged BNIP3 (WT)
Lane 3: His-tagged BNIP3 (ΔTM)

Figure 23: Western blot for proteins lysed from HEK293 cells transfected with pcDNA3 vector, HA-tagged wild-type (WT) BNIP3 or His-tagged ΔTM BNIP3. (A) Blot was probed with mouse anti-HA-tag antibody. (B) Blot was probed with mouse anti-His-tag antibody. (C) Blot was probed with rabbit anti-BNIP3 antibody.

I then examined total cell death over 48 hours in HEK293 cells transfected with empty pcDNA3 vector or ΔTM BNIP3 over-expression vector and treated with 400 μM hydrogen peroxide (Figure 24B). Measurements were again taken by staining with AO/EtBr and counting manually on a fluorescent microscope. Average cell death was significantly lower in ΔTM BNIP3 cells than in control cells at 18 and 24 hours of treatment, but not at 48 hours of treatment or at less than 18 hours of treatment.

To more accurately determine the level of cell death in HEK293 cells transfected with pcDNA3 and ΔTM BNIP3 vectors, I treated cells with a range of hydrogen peroxide concentrations over 24 hours and measured total cell death by flow cytometry with trypan blue staining (Figure 24C). I found that average cell death with treatment was not significantly different between control and ΔTM BNIP3 cells at any of the treatment concentrations.

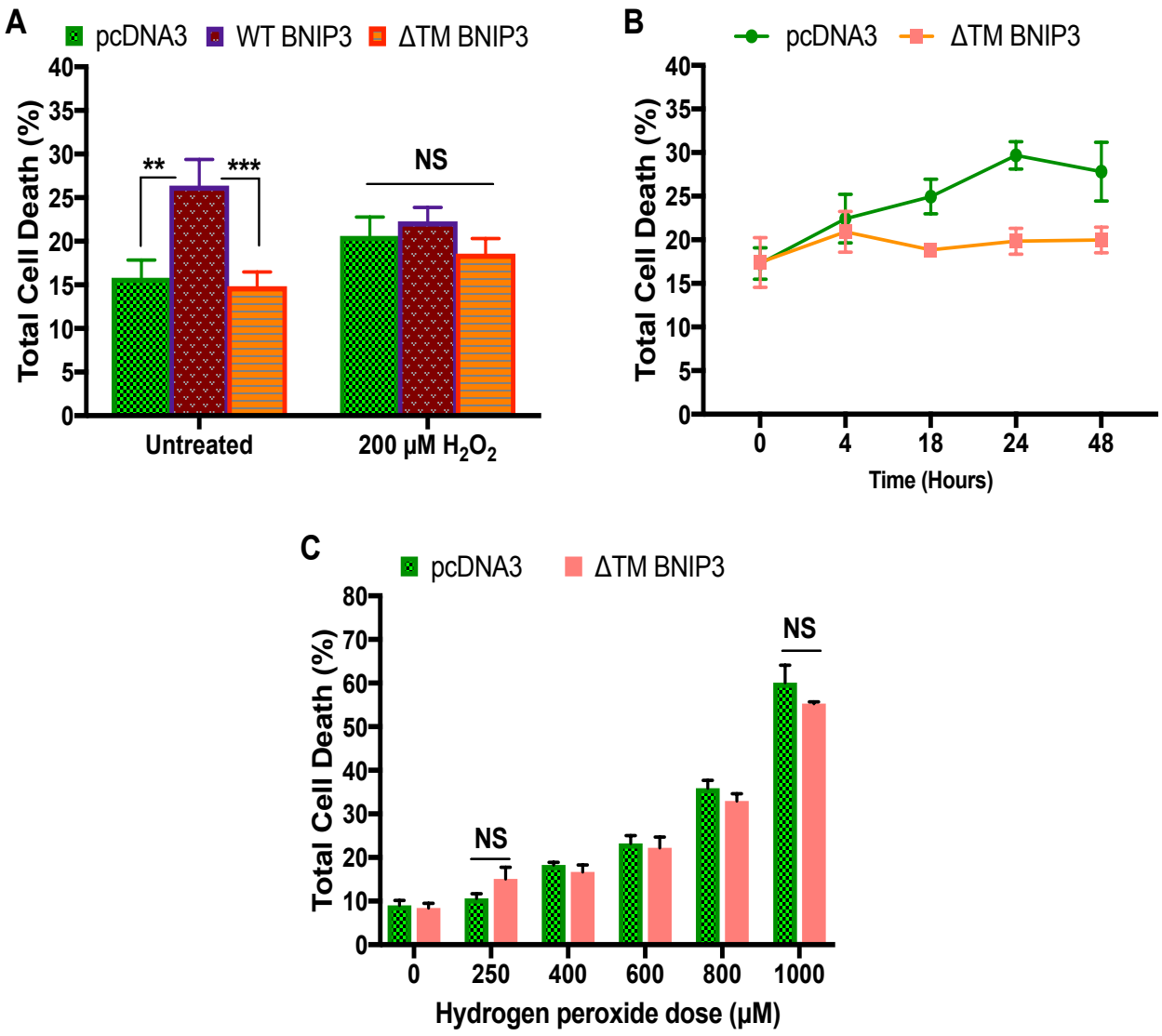

Figure 24: Total cell death for HEK293 cells transfected with pcDNA3 or BNIP3 over-expression vectors.
(A) Mean cell death for HEK293 cells transfected with pcDNA3, WT BNIP3 or ΔTM BNIP3 and treated with 200μM hydrogen peroxide for 24 hours. Measurements were by AO/EtBr counts on a fluorescent microscope. N=5, n=2.
(B) Mean cell death for HEK293 cells transfected with pcDNA3 or ΔTM BNIP3 and treated with 400μM hydrogen peroxide over 48 hours. Significance is pcDNA3 versus ΔTM BNIP3 for each condition. Measurements were AO/EtBr counts. N=2, n=2. Statistical analysis was not performed.
(C) Mean cell death for HEK293 cells transfected with pcDNA3 or ΔTM BNIP3 and treated with 0-1000μM hydrogen peroxide for 24 hours. N=5, n=3. There were no significant differences between the means.
Bars represent standard error.

To determine whether endogenous BNIP3 caused oxidative stress-induced cell death, I transfected HEK293 cells with siRNA against BNIP3 to reduce its levels. I confirmed knockdown of BNIP3 by collecting cell lysates 48 hours after transfection and western blotting for BNIP3 levels (Figure 25A). I then treated knockdown and control cells with hydrogen peroxide for 24 hours and measured death by flow cytometry (Figure 25B). I found that BNIP3 knockdown significantly decreased average cell death in cells treated with both 400 μM hydrogen peroxide (11.2% vs. 19.9% death in control cells) and 600 μM hydrogen peroxide (13.9% vs. 18.2% death in control cells), as well as providing a slight reduction in death in untreated cells (9.4% vs. 12.9% death in control cells). Mean cell death was not significantly different between knockdown and control cells at higher concentrations of hydrogen peroxide treatment.

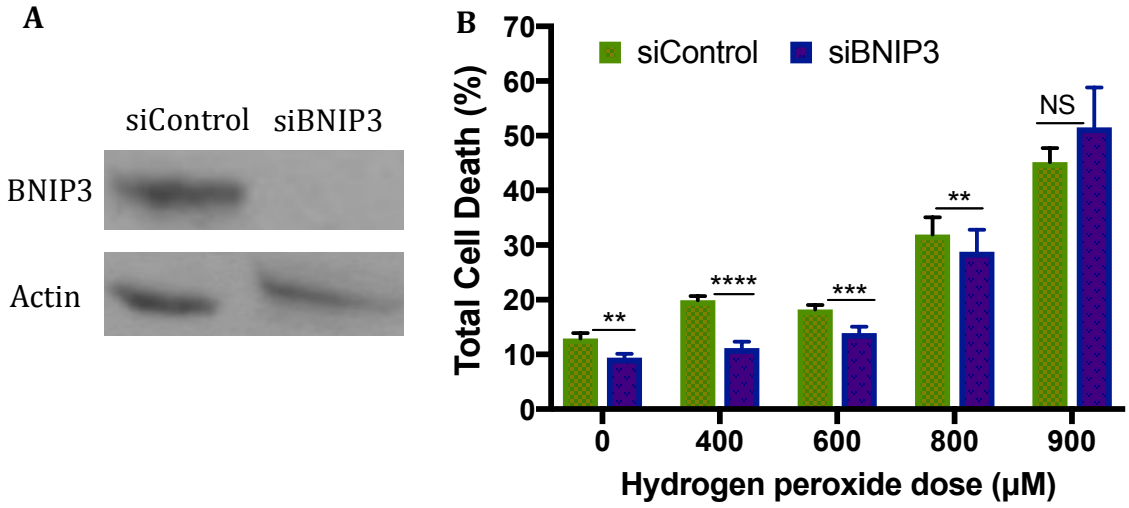

Figure 25: BNIP3 knockdown provides some protection against cell death in HEK293 cells. (A) Western blot for BNIP3 levels in HEK293 cells transfected with siRNA scramble control (siControl) or pooled siRNA against BNIP3 (siBNIP3). β-Actin was probed for as a loading control. N=1. (B) Mean cell death in HEK293 cells transfected with siRNA and then treated with hydrogen peroxide for 24 hours, as measured by flow cytometry with trypan blue staining. N=3, n=3. Bars represent standard error.

Finally, to confirm the effects of endogenous BNIP3 on oxidative stress-induced cell death I used Murine Embryonic Fibroblast (MEF) cells that either expressed wild-type BNIP3 (WT MEF) or did not express BNIP3 protein (KO MEF). I treated these cells with a range of hydrogen peroxide concentrations for 24 hours and then measured total cell death by flow cytometry with trypan blue staining (Figure 26). Mean cell death was moderately but significantly lower in BNIP3 knockout MEF cells than in BNIP3 wild-type MEF when treated with 200 - 800 µM hydrogen peroxide (9.79% vs. 12.87% at 200 µM; 19.64% vs. 25.72% at 400 µM; 35.89 vs. 44.67% at 600 µM; 70.61 vs. 84.59% at 800 µM), with the 800 µM treatment condition displaying the most meaningful difference. Mean cell death was not meaningfully different in BNIP3 knockout MEF cells than in WT cells when treated with 1000 µM hydrogen peroxide (93.12% vs. 92.79%).

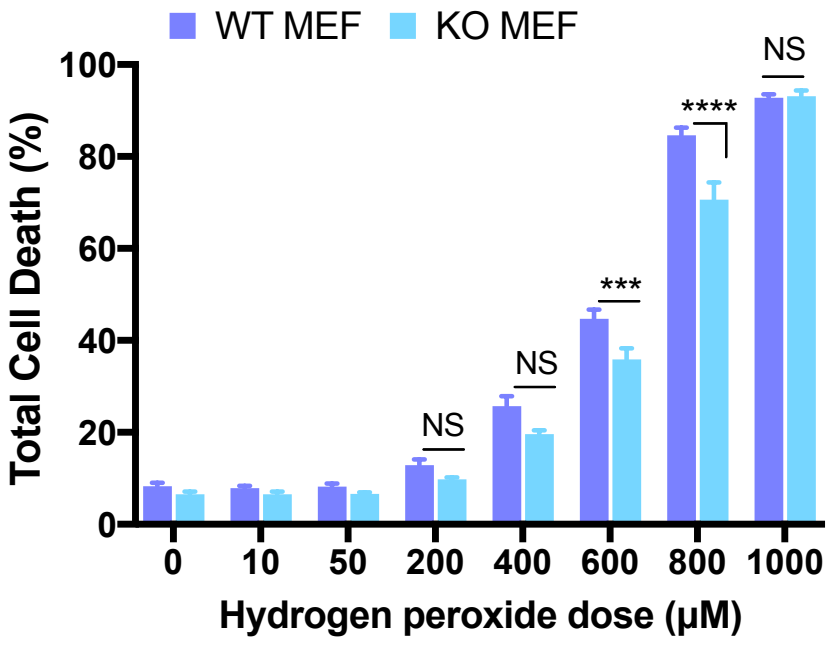

Figure 26: Loss of BNIP3 moderately decreases oxidative stress-induced cell death. Mean cell death on BNIP3 wild-type (WT) and knockout (KO) Murine Embryonic Fibroblast (MEF) cells treated with hydrogen peroxide for 24 hours, as measured by flow cytometry with trypan blue staining. N=5, n=3. Bars represent standard error.

Chapter 4: Discussion and Conclusion

In this study hydrogen peroxide treatment was used to induce oxidative stress in the transformed human embryonic kidney cell line HEK293 and the human glioblastoma cell line U87. Oxidative stress-induced cell death increased in both a time-dependent and dose-dependent manner, as expected from treatment with a molecule known to damage proteins, lipids and DNA[87,88,92]. U87 cells were somewhat more resistant to oxidative stress induced cell death at the highest treatment levels than HEK293 cells, which is consistent with the fact that resisting cell death is a hallmark of cancer[120]. The reduction in cell death at higher doses of hydrogen peroxide could potentially be attributed to molecular differences between the two cell lines.

Internal levels of both superoxide and hydrogen peroxide increased in both cell lines after treatment with hydrogen peroxide. While relative quantities of both species increased appreciably in HEK293 cells, a dramatic increase was seen in internal hydrogen peroxide levels in U87 cells. Cancer cells often have high levels of ROS and increased antioxidant activity[87], which may explain this observation. Damage caused by ROS would increase superoxide production at mitochondria and other sites[88], leading to increased hydrogen peroxide due to rapid conversion by antioxidant systems. Intracellular staining for mitochondrial membrane potential with and without hydrogen peroxide treatment in HEK293 cells confirmed that the treatment disrupted mitochondrial function.

BNIP3 protein dimers increased with a 24-hour hydrogen peroxide treatment in HEK293 cells, with a slight upward trend that may be dose-dependent but was not statistically significant. The BNIP3 monomer was not present in measureable quantities. In

contrast, BNIP3 protein dimers in U87 cells did not show a clear trend in expression, whereas BNIP3 monomers appeared to decrease with hydrogen peroxide treatment. As BNIP3 dimers are resistant to both detergent and reducing conditions I was unable to measure total protein levels in either cell line, making it impossible to determine from the quantified blots whether BNIP3 protein levels changed overall in U87 cells. A decrease in protein levels caused by increased proteasomal degradation could be examined using the proteasome inhibitor MG132, but that avenue was not explored during this study.

Similar to the western blot results, qPCR for *BNIP3* mRNA in HEK293 cells revealed a small increase in levels after 5 hours treatment with hydrogen peroxide, indicating a weak induction of gene expression. The 5-hour time point was selected to observe relevant increases in gene expression prior to the increased protein expression seen at 24 hours. However, it is possible that greater upregulation of mRNA would have been seen at a different time point. BNIP3 is known to be over-expressed in glioblastoma[17], suggesting that mRNA levels should also be high in the U87 glioblastoma cell line. However, as I did not measure *BNIP3* mRNA levels in U87 cells, I cannot comment on whether these levels increase with hydrogen peroxide treatment.

Immunofluorescent staining for BNIP3 and mitochondria in HEK293 after hydrogen peroxide treatment shows an increase of BNIP3 fluorescence and colocalization with mitochondria with treatment, suggesting that oxidative stress leads to increased mitochondrial localization of BNIP3 in HEK293 cells. BNIP3 fluorescence also increases in U87 cells when treated with lower hydrogen peroxide concentrations (50 and 200 μM), but not in cells treated with higher concentrations. Similarly, Pearson's correlation coefficient suggests there may be a slight increase in colocalization of BNIP3 with mitochondria when

U87 cells are treated with 200 μM hydrogen peroxide but not with higher concentrations. However, this increase is not statistically significant compared to untreated cells. Both treated and untreated U87 cells showed considerable partial colocalization of BNIP3 with mitochondria, with the majority of mitochondrial fluorescence colocalizing with BNIP3 fluorescence according to the Manders' coefficient. These results show that some amount of BNIP3 protein is already present at mitochondria in untreated cells, and that acute oxidative stress does not appreciably alter this fact. BNIP3 is also noticeably present in the nucleus of U87 cells, which is consistent with the fact that BNIP3 is expressed in the nucleus of glial cells[67]. It is possible that nuclear BNIP3 is contributing to a survival response in U87 cells during oxidative stress, reducing somewhat the level of death seen in U87 cells compared to HEK293 cells.

As splice variant BNIP3 is known to act as a dominant negative against full length BNIP3[33], I over-expressed a truncated BNIP3 protein that should act similarly, in order to explore BNIP3's role in oxidative stress-induced cell death. I found that over-expression of ΔTM BNIP3 had little effect on survival of HEK293 cells treated with hydrogen peroxide. The transfection efficiency was approximately 80% at 48 hours after transfection, but it is possible that the over-expression vector did not function as intended. However, full length BNIP3 may not be responsible for death during acute oxidative stress, in which case inhibition of its function would not decrease cell death.

Silencing of BNIP3 expression in HEK293 cells using siRNA resulted in a statistically significant decrease in cell death, although the decrease was minor and was not observed at the highest treatment concentrations. Likewise, hydrogen peroxide treatment of BNIP3 knockout MEF cells lead to a minor decrease in cell death compared to BNIP3 wild-type

cells. These observations suggest that BNIP3 is not the main actor in oxidative stress induced cell death.

If that is the case, we must question why BNIP3 mitochondrial localization increases in HEK293 cells following hydrogen peroxide treatment, and what function it is performing there. It is likely that oxidative stress causes mitochondrial damage, leading BNIP3 to mediate mitophagy (autophagic removal of mitochondria)[43]. For some cells, BNIP3 may also induce cell death. However, BNIP3 induction of cell death is weak compared to other BCL2 family members[20,30,37,38]. Thus it would be reasonable for cellular response to acute and highly damaging oxidative stress conditions to involve mediation of cell death by more potent regulators such as BAX and BAK.

In conclusion, this study demonstrates that acute oxidative stress increases cell death, upregulates BNIP3 expression and increases colocalization of BNIP3 with mitochondria in HEK293 cells, but only increases cell death in U87 cells. It does not appear that acute oxidative stress has an affect on BNIP3 expression or localization in U87 cells. Overall, BNIP3 may participate in acute oxidative stress induced cell death, but is not required for it in HEK293 cells, U87 cells, or in MEFs.

Chapter 5: Future Directions

While this study sought to investigate the effects of acute oxidative stress on the expression, localization, and function of BNIP3, future research should explore the effects of chronic, low level oxidative stress. A review of the literature shows that several studies have demonstrated an increase in BNIP3 expression upon treatment with hydrogen peroxide[27,54,121]. An experiment that treated hepatoma cells with 25 or 40 μM hydrogen peroxide every 15 minutes for 2 hours resulted in stabilization of HIF1α[122], suggesting that repeated application of hydrogen peroxide could lead to upregulation of BNIP3 expression. As BNIP3 induction of cell death is delayed compared to other family members[20,30,37,38], the protein is far more likely to play an important role in cellular response to ongoing stress.

Considering that acute oxidative stress led to disruption of mitochondrial membrane potential while increasing mitochondrial localization of BNIP3 in HEK293 cells, it is also possible that BNIP3 may regulate mitochondrial membrane integrity. Future experiments could explore this possibility using mitochondrial dyes with hydrogen peroxide treatment and knockdown of BNIP3, and by western blotting for release of executioner proteins such as cytochrome c and caspases from mitochondria.

This study also did not determine the type of cell death that was induced by acute oxidative stress in HEK293 and U87 cell lines. Future experiments should investigate the cell death type using inhibitors against apoptosis and autophagy, as well as whether proteins involved in autophagy and apoptosis were upregulated or activated in response to hydrogen peroxide treatment. Some preliminary exploration suggested that levels of the autophagy protein beclin1 increase with hydrogen peroxide treatment in a dose-dependent

manner in HEK293 cells, but further experimentation is needed to confirm whether autophagy levels change with hydrogen peroxide treatment and whether autophagy is contributing to cell death or survival.

Additional experimentation using non-cancerous glial cells such as murine astrocytes, as well as other glioblastoma cell lines or brain tumour initiating cells, would be beneficial to confirming the role of BNIP3 in oxidative stress-induced cell death in both cancerous and non-cancerous brain cells. Measurement of *BNIP3* mRNA levels with and without hydrogen peroxide treatment, and of BNIP3 protein levels under oxidative stress with and without the proteasome inhibitor MG132, would also be helpful to strengthen the conclusions of this study.

Chapter 6: References

1. Chi X, Kale J, Leber B, Andrews DW. Regulating cell death at, on, and in membranes. *Biochim Biophys Acta*. 2014;1843:2100-2113. doi:10.1016/j.bbamcr.2014.06.002.
2. Qi Y, Tian X, Liu J, et al. Bnip3 and AIF cooperate to induce apoptosis and cavitation during epithelial morphogenesis. *J Cell Biol*. 2012;198(1):103-114. doi:10.1083/jcb.201111063.
3. Ashkenazi A. Targeting the extrinsic apoptotic pathway in cancer: lessons learned and future directions. *J Clin Invest*. 2015;125(2):487-489. doi:10.1172/JCI80420.normal.
4. Ashkenazi A, Salvesen G. Regulated Cell Death: Signaling and Mechanisms. *Annu Rev Cell Dev Biol*. 2014;30:337-356. doi:10.1146/annurev-cellbio-100913-013226.
5. Siddiqui WA, Ahad A, Ahsan H. The mystery of BCL2 family: Bcl - 2 proteins and apoptosis: an update. *Arch Toxicol*. 2015;89:289-317. doi:10.1007/s00204-014-1448-7.
6. Gross A. BCL-2 family proteins as regulators of mitochondria metabolism. *Biochim Biophys Acta*. 2016;1857:1243-1246. doi:10.1016/j.bbabio.2016.01.017.
7. Lomonosova E, Chinnadurai G. BH3-only proteins in apoptosis and beyond: an overview. *Oncogene*. 2008;27(Suppl 1):S2-19. doi:10.1038/onc.2009.39.BH3-only.
8. Shamas-Din A, Kale J, Leber B, Andrews DW. Mechanisms of Action of Bcl-2 Family Proteins. *Cold Spring Harb Perspect Biol*. 2013;5:1-21.

9. Boyd JM, Malstrom S, Subramanian T, Venkatesh LK, Schaeper U, Elangovan B. Adenovirus El B 19 kDa and Bcl-2 Proteins Interact with a Common Set of Cellular Proteins. *Cell*. 1994;79:341-351.

10. Han J, Sabbatini P, Perez D, Rao L, Modha D, White E. The E1B 19K protein blocks apoptosis by Interacting with and inhibiting the p53-inducible and death-promoting Bax protein. *Genes Dev*. 1996;10:461-477.

11. White E. Regulation of the cell cycle and apoptosis by the oncogenes of adenovirus. *Oncogene*. 2001;20:7836-7846.

12. Cuconati A, White E. Viral homologs of BCL-2: role of apoptosis in the regulation of virus infection. *Genes Dev*. 2002;16:2465-2478. doi:10.1101/gad.1012702.sis.

13. Chen G, Cizeau J, Velde C Vande, et al. Nix and Nip3 Form a Subfamily of Pro-apoptotic Mitochondrial Proteins. *J Biol Chem*. 1999;274(1):7-10. doi:10.1074/jbc.274.1.7.

14. Gross MB. Personal Communication in OMIM® Online Mendelian Inheritance in Man. MIM number: {603293} Johns Hopkins University, Baltimore, MD. https://omim.org/. Published 2011.

15. Gang H, Dhingra R, Lin J, et al. PDK2-mediated alternative splicing switches Bnip3 from cell death to cell survival. *J Cell Biol*. 2015;210(7):1101-1115. doi:10.1083/jcb.201504047.

16. Chen BG, Ray R, Dubik D, et al. The E1B 19K/Bcl-2-binding Protein Nip3 is a Dimeric Mitochondrial Protein that Activates Apoptosis. *J Exp Med*. 1997;186(12):1975-1983.

17. Burton TR, Gibson SB. The role of Bcl-2 family member BNIP3 in cell death and disease: NIPping at the heels of cell death. *Cell Death Differ*. 2009;16(4):515-523. doi:10.1038/cdd.2008.185.

18. Lawriea CM, Sulistijoa ES, MacKenzie KR. Intermonomer hydrogen bonds enhance GxxxG-driven dimerization of the BNIP3 transmembrane domain: roles for sequence context in helix-helix association in membranes. *J Mol Biol*. 2010;396(4):924-936. doi:10.1016/j.jmb.2009.12.023.Intermonomer.

19. Vasagiri N, Kutala VK. Structure, function, and epigenetic regulation of BNIP3: A pathophysiological relevance. *Mol Biol Rep*. 2014;41(11):7705-7714. doi:10.1007/s11033-014-3664-x.

20. Yasuda M, Theodorakis P, Subramanian T, Chinnadurai G. Adenovirus E1B-19K/BCL-2 Interacting Protein BNIP3 Contains a BH3 Domain and a Mitochondrial Targeting Sequence. *J Biol Chem*. 1998;273(20):12415-12421.

21. Ray R, Chen G, Vande Velde C, et al. BNIP3 Heterodimerizes with Bcl-2/Bcl-X L and Induces Cell Death Independent of a Bcl-2 Homology 3 (BH3) Domain at Both Mitochondrial and Nonmitochondrial Sites. *J Biol Chem*. 2000;275(2):1439-1448. doi:10.1074/jbc.275.2.1439.

22. Sulistijo ES, Jaszewski TM, Mackenzie KR. Sequence-specific Dimerization of the Transmembrane Domain of the "BH3-only" Protein BNIP3 in Membranes and Detergent. *J Biol Chem*. 2003;278(51):51950-51956. doi:10.1074/jbc.M308429200.

23. Vereshaga YA, Volynsky PE, Pustovalova JE, Nolde DE, Arseniev AS, Efremov RG. Specificity of helix packing in transmembrane dimer of the cell death factor BNIP3: A molecular modeling study. *Proteins*. 2007;69:309-325. doi:10.1002/prot.

24. Kim J, Cho J, Ha J, Park J. The Carboxy Terminal C-Tail of BNip3 Is Crucial in Induction of Mitochondrial Permeability Transition in Isolated Mitochondria. *Arch Biochem Biophys*. 2002;398(2):147-152. doi:10.1006/abbi.2001.2673.

25. Bocharov E V., Pustovalova YE, Pavlov K V., et al. Unique Dimeric Structure of BNip3 Transmembrane Domain Suggests Membrane Permeabilization as a Cell Death Trigger. *J Biol Chem*. 2007;282(22):16256-16266. doi:10.1074/jbc.M701745200.

26. Sulistijo ES, Mackenzie KR. Structural Basis for Dimerization of the BNIP3 Transmembrane Domain. *Biochemistry*. 2009;48(23):5106-5120. doi:10.1021/bi802245u.

27. Kubli DA, Quinsay MN, Huang C, Lee Y, Gustafsson ÅB. Bnip3 functions as a mitochondrial sensor of oxidative stress during myocardial ischemia and reperfusion. *Am J Physiol - Hear Circ Physiol*. 2008;295:2025-2031. doi:10.1152/ajpheart.00552.2008.

28. Hanna RA, Quinsay MN, Orogo AM, Giang K, Rikka S, Gustafsson ÅB. Microtubule-associated Protein 1 Light Chain 3 (LC3) Interacts with Bnip3 Protein to Selectively Remove Endoplasmic Reticulum and Mitochondria via Autophagy. *J Biol Chem*. 2012;287(23):19094-19104. doi:10.1074/jbc.M111.322933.

29. Vande Velde C, Cizeau J, Dubik D, et al. BNIP3 and Genetic Control of Necrosis-Like Cell Death through the Mitochondrial Permeability Transition Pore. *Mol Cell Biol*. 2000;20(15):5454-5468. doi:10.1128/MCB.20.15.5454-5468.2000.

30. Chinnadurai G, Vijayalingam S, Gibson S. BNIP3 subfamily BH3-only proteins: mitochondrial stress sensors in normal and pathological functions. *Oncogene*. 2009;27(S1):S114-S127. doi:10.1038/onc.2009.49.BNIP3.

31. Kothari S, Cizeau J, Mcmillan-ward E, et al. BNIP3 plays a role in hypoxic cell death in human epithelial cells that is inhibited by growth factors EGF and IGF. *Oncogene*. 2003;22:4734-4744. doi:10.1038/sj.onc.1206666.

32. Park CW, Hong SM, Kim E, et al. BNIP3 is degraded by ULK1-dependent autophagy via MTORC1 and AMPK. *Autophagy*. 2013;9(3):345-360. doi:10.4161/auto.23072.

33. Bristow N, Burton TR, Henson ES, Ong-Justiniano C, Brown M, Gibson SB. Truncated forms of BNIP3 act as dominant negatives inhibiting hypoxia-induced cell death. *Biochim Biophys Acta - Mol Basis Dis*. 2011;1812(3):302-311. doi:10.1016/j.bbadis.2010.11.013.

34. Zhu Y, Massen S, Terenzio M, et al. Modulation of serines 17 and 24 in the LC3-interacting region of Bnip3 determines pro-survival mitophagy versus apoptosis. *J Biol Chem*. 2013;288(2):1099-1113. doi:10.1074/jbc.M112.399345.

35. Rogers S, Wells R, Rechsteiner M. Amino Acid Sequences Common to Rapidly Degraded Proteins: The PEST Hypothesis. *Science (80-)*. 1986;234(4774):364-368.

36. Choe SC, Hamacher-Brady A, Brady NR. Autophagy capacity and sub-mitochondrial heterogeneity shape Bnip3-induced mitophagy regulation of apoptosis. *Cell Commun Signal*. 2015;13:37. doi:10.1186/s12964-015-0115-9.

37. Rikka S, Quinsay MN, Thomas RL, et al. Bnip3 impairs mitochondrial bioenergetics and stimulates mitochondrial turnover. *Cell Death Differ*. 2011;18(4):721-731. doi:10.1038/cdd.2010.146.

38. Zhang J, Ney PA. Role of BNIP3 and NIX in cell death, autophagy, and mitophagy. *Cell Death Differ*. 2009;16(7):939-946. doi:10.1038/cdd.2009.16.ROLE.

39. Glick D, Zhang W, Beaton M, et al. BNip3 Regulates Mitochondrial Function and Lipid Metabolism in the Liver. *Mol Cell Biol*. 2012;32(13):2570-2584. doi:10.1128/MCB.00167-12.

40. Gustafsson AB. Bnip3 as a Dual Regulator of Mitochondrial Turnover and Cell Death in the Myocardium. *Pedriatric Cardiol*. 2011;32:267-274. doi:10.1007/s00246-010-9876-5.

41. Quinsay MN, Lee Y, Rikka S, et al. Bnip3 Mediates Permeabilization of Mitochondria and Release of Cytochrome c via a Novel Mechanism. *J Mol Cell Cardiol*. 2010;48(6):1146-1156. doi:10.1016/j.yjmcc.2009.12.004.

42. Liu KE, Frazier WA. Phosphorylation of the BNIP3 C-Terminus Inhibits Mitochondrial Damage and Cell Death without Blocking Autophagy. *PLoS One*. 2015;10(6):e0129667. doi:10.1371/journal.pone.0129667.

43. Thomas RL, Kubli DA, Gustafsson ÅB. Bnip3-mediated defects in oxidative phosphorylation promote mitophagy. *Autophagy*. 2011;7(7):775-777. doi:10.4161/auto.7.7.15536.

44. Regula KM, Ens K, Kirshenbaum LA. Inducible Expression of BNIP3 Provokes Mitochondrial Defects and Hypoxia-Mediated Cell Death of Ventricular Myocytes. *Circ Res*. 2002;91(3):226-231. doi:10.1161/01.RES.0000029232.42227.16.

45. Landes T, Emorine LJ, Courilleau D, Rojo M, Belenguer P, Arnaune-Pelloquin L. The BH3-only Bnip3 binds to the dynamin Opa1 to promote mitochondrial fragmentation and apoptosis by distinct mechanisms. *EMBO Rep*. 2010;11(6):459-465. doi:10.1038/embor.2010.50.

46. Lee Y, Lee H, Hanna RA, Gustafsson ÅB. Mitochondrial autophagy by Bnip3 involves Drp1-mediated mitochondrial fission and recruitment of Parkin in cardiac myocytes. *Am J Physiol - Hear Circ Physiol*. 2011;301:1924-1931. doi:10.1152/ajpheart.00368.2011.

47. Kubli DA, Ycaza JE, Gustafsson AB. Bnip3 mediates mitochondrial dysfunction and cell death through Bax and Bak. *Biochem J*. 2007;405:407-415. doi:10.1042/BJ20070319.

48. Hendgen-Cotta UB, Esfeld S, Rudi K, Miinalainen I, Klare JP, Rassaf T. Cytosolic BNIP3 Dimer Interacts with Mitochondrial BAX Forming Heterodimers in the Mitochondrial Outer Membrane under Basal Conditions. *Int J Mol Sci*. 2017;18(4):E687. doi:10.3390/ijms18040687.

49. Quinsay MN, Thomas RL, Lee Y, Gustafsson ÅB. Bnip3-mediated mitochondrial autophagy is independent of the mitochondrial permeability transition pore. *Autophagy*. 2010;6(7):855-862. doi:10.4161/auto.6.7.13005.

50. Zhang X, Bian X, Kong J. The proapoptotic protein BNIP3 interacts with VDAC to induce mitochondrial release of endonuclease G. *PLoS One*. 2014;9(12):1-14. doi:10.1371/journal.pone.0113642.

51. Zhang Z, Yang X, Zhang S, Ma X, Kong J. BNIP3 Upregulation and EndoG Translocation in Delayed Neuronal Death in Stroke and in Hypoxia. *Stroke*. 2007;38(5):1606-1613. doi:10.1161/STROKEAHA.106.475129.

52. Graham RM, Thompson JW, Webster K a. Inhibition of the vacuolar ATPase induces Bnip3-dependent death of cancer cells and a reduction in tumor burden and metastasis. *Oncotarget*. 2014;5(5):1162-1173.

53. Chen Y, McMillan-Ward E, Kong J, Israels SJ, Gibson SB. Oxidative stress induces autophagic cell death independent of apoptosis in transformed and cancer cells. *Cell Death Differ*. 2008;15(1):171-182. doi:10.1038/sj.cdd.4402233.

54. Byun YJ, Kim SK, Kim YM, Chae GT, Jeong SW, Lee SB. Hydrogen peroxide induces autophagic cell death in C6 glioma cells via BNIP3-mediated suppression of the mTOR pathway. *Neurosci Lett*. 2009;461(2):131-135. doi:10.1016/j.neulet.2009.06.011.

55. Hetschko H, Voss V, Senft C, Seifert V, Prehn JHM, Kögel D. BH3 Mimetics Reactivate Autophagic Cell Death in Anoxia-Resistant Malignant Glioma Cells. *Neoplasia*. 2008;10(8):873-885. doi:10.1593/neo.07842.

56. Liu Y, Levine B. Autosis and autophagic cell death: the dark side of autophagy. *Cell Death Differ*. 2015;22(3):367-376. doi:10.1038/cdd.2014.143.

57. Yin Z, Pascual C, Klionsky DJ. Autophagy: machinery and regulation. *Microb Cell*. 2016;3(12):588-596. doi:10.15698/mic2016.12.546.

58. Parzych KR, Klionsky DJ. An Overview of Autophagy: Morphology, Mechanism, and Regulation. *Antioxidants Redox Signal*. 2014;20(3):460-473. doi:10.1089/ars.2013.5371.

59. Harnett MM, Pineda MA, Latre de Late P, et al. From Christian de Duve to Yoshinori Ohsumi: More to autophagy than just dining at home. *Biomed J*. 2017;40:9-22. doi:10.1016/j.bj.2016.12.004.

60. Li Y, Wang Y, Kim E, et al. Bnip3 Mediates the Hypoxia-induced Inhibition on Mammalian Target of Rapamycin by Interacting with Rheb. *J Biol Chem*. 2007;282(49):35803-35813. doi:10.1074/jbc.M705231200.

61. Lin A, Yao J, Zhuang L, et al. FoxO-BNIP3 axis exerts a unique regulation of mTORC1 and cell survival under energy stress. *Oncogene*. 2014;33(24):3183-3194. doi:10.1038/onc.2013.273.FoxO-BNIP3.

62. Decuypere J-P, Parys JB, Bultynck G. Regulation of the autophagic bcl-2/beclin 1 interaction. *Cells*. 2012;1(3):284-312. doi:10.3390/cells1030284.

63. Zhang T, Xue L, Li L, et al. BNIP3 Protein Suppresses PINK1 Kinase Proteolytic Cleavage to Promote Mitophagy. *J Biol Chem*. 2016;291(41):21616-21629. doi:10.1074/jbc.M116.733410.

64. Shi R-Y, Zhu S-H, Li V, Gibson SB, Xu X-S, Kong J-M. BNIP3 Interacting with LC3 Triggers Excessive Mitophagy in Delayed Neuronal Death in Stroke. *CNS Neurosci Ther*. 2014;20:1045-1055. doi:10.1111/cns.12325.

65. Pickrell AM, Youle RJ. The Roles of PINK1, Parkin and Mitochondrial Fidelity in Parkinson's Disease. *Neuron*. 2016;85(2):257-273. doi:10.1016/j.neuron.2014.12.007.The.

66. Kubli DA, Cortez MQ, Moyzis AG, Najor RH, Lee Y, Gustafsson AB. PINK1 Is Dispensable for Mitochondrial Recruitment of Parkin and Activation of Mitophagy in Cardiac Myocytes. *PLoS One*. 2015;10(6):e130707. doi:10.1371/journal.pone.0130707.

67. Burton TR, Henson ES, Baijal P, Eisenstat DD, Gibson SB. The pro-cell death Bcl-2 family member, BNIP3, is localized to the nucleus of human glial cells: Implications for glioblastoma multiforme tumor cell survival under hypoxia. *Int J Cancer*. 2006;118:1660-1669. doi:10.1002/ijc.21547.

68. Burton TR, Eisenstat DD, Gibson SB. BNIP3 (Bcl-2 19 kDa Interacting Protein) Acts as Transcriptional Repressor of Apoptosis-Inducing Factor Expression Preventing Cell Death in Human Malignant Gliomas. *J Neurosci*. 2009;29(13):4189-4199. doi:10.1523/JNEUROSCI.5747-08.2009.

69. Burton T, Henson E, Azad M, Brown M, Eisenstat D, Gibson S. BNIP3 acts as transcriptional repressor of death receptor-5 expression and prevents TRAIL-induced cell death in gliomas. *Cell Death Dis*. 2013;4:e587. doi:10.1038/cddis.2013.100.

70. Gang H, Hai Y, Dhingra R, et al. A Novel Hypoxia-Inducible Spliced Variant of Mitochondrial Death Gene Bnip3 Promotes Survival of Ventricular Myocytes. *Circ Res*. 2011;108:1084-1092. doi:10.1161/CIRCRESAHA.110.238709.

71. Yasuda M, Han J, Dionne CA, Boyd JM, Chinnadurai G. BNIP3α: A Human Homolog of Mitochondrial Proapoptotic Protein BNIP3. *Cancer Res*. 1999;59:533-537.

72. Sowter HM, Ratcliffe PJ, Watson P, Greenberg AH, Harris AL. HIF-1-dependent regulation of hypoxic induction of the cell death factors BNIP3 and NIX in human tumors. *Cancer Res*. 2001;61(18):6669-6673.

73. Zhang HM, Cheung P, Yanagawa B, McManus BM, Yang DC. BNips: A group of pro-apoptotic proteins in the Bcl-2 family. *Apoptosis*. 2003;8(3):229-236.

74. Hamacher-Brady A, Brady N, Logue S, et al. Response to myocardial ischemia/reperfusion injury involves Bnip3 and autophagy. *Cell Death Differ*. 2007;14:146-157. doi:10.1038/sj.cdd.4401936.

75. Bruick RK. Expression of the gene encoding the proapoptotic Nip3 protein is induced by hypoxia. *PNAS*. 2000;97(16):9082-9087.

76. Wheaton WW, Chandel NS. Hypoxia regulates cellular metabolism. *Am J Physiol Cell Physiol*. 2011;300:C385-C393. doi:10.1152/ajpcell.00485.2010.

77. Kumar H, Choi D. Hypoxia Inducible Factor Pathway and Physiological Adaptation: A Cell Survival Pathway? *Mediators Inflamm*. 2015;2015:1-11. doi:10.1155/2015/584758.

78. Muz B, de la Puente P, Azab F, Azab AK. The role of hypoxia in cancer progression, angiogenesis, metastasis, and resistance to therapy. *Hypoxia*. 2015;3:83-92.

79. Niecknig H, Tug S, Reyes BD, Kirsch M, Berchner-pfannschmidt U. Role of reactive oxygen species in the regulation of HIF-1 by prolyl hydroxylase 2 under mild hypoxia. *Free Radic Res*. 2012;46(6):705-717. doi:10.3109/10715762.2012.669041.

80. Chourasia AH, Macleod KF. Tumor suppressor functions of BNIP3 and mitophagy. *Autophagy*. 2015;11(10):1937-1938. doi:10.1080/15548627.2015.1085136.

81. Pratt J, Annabi B. Induction of autophagy biomarker BNIP3 requires a JAK2/STAT3 and MT1-MMP signaling interplay in Concanavalin-A-activated U87 glioblastoma cells. *Cell Signal*. 2014;26(5):917-924. doi:10.1016/j.cellsig.2014.01.012.

82. Mammucari C, Milan G, Romanello V, et al. FoxO3 Controls Autophagy in Skeletal Muscle In Vivo. *Cell Metab*. 2007;6(6):458-471. doi:10.1016/j.cmet.2007.11.001.

83. You L, Wang Z, Li H, et al. The role of STAT3 in autophagy. *Autophagy*. 2015;11(5):729-739. doi:10.1080/15548627.2015.1017192.

84. Tracy K, Dibling BC, Spike BT, Knabb JR, Schumacker P, Macleod KF. BNIP3 Is an RB/E2F Target Gene Required for Hypoxia-Induced Autophagy. *Mol Cell Biol*. 2007;27(17):6229-6242. doi:10.1128/MCB.02246-06.

85. Pereira EJ, Smolko CM, Janes KA. Computational Models of Reactive Oxygen Species as Metabolic Byproducts and Signal-Transduction Modulators. *Front Pharmacol*. 2016;7:1-9. doi:10.3389/fphar.2016.00457.

86. Nathan C, Cunningham-Bussel A. Beyond oxidative stress: an immunologist's guide to reactive oxygen species. *Nat Rev Immunol*. 2013;13(5):349-361. doi:10.1038/nri3423.

87. Schieber M, Chandel NS. ROS Function in Redox Signaling and Oxidative Stress. *Curr Biol*. 2014;24(10):1-25. doi:10.1016/j.cub.2014.03.034.ROS.

88. Liemburg-Apers DC, Willems PHGM, Koopman WJH, Grefte S. Interactions between mitochondrial reactive oxygen species and cellular glucose metabolism. *Arch Toxicol*. 2015;89(8):1209-1226. doi:10.1007/s00204-015-1520-y.

89. Wen X, Wu J, Wang F, Liu B, Huang C, Wei Y. Deconvoluting the role of reactive oxygen species and autophagy in human diseases. *Free Radic Biol Med*. 2013;65:402-410. doi:10.1016/j.freeradbiomed.2013.07.013.

90. Brown DI, Griendling KK. Regulation of signal transduction by reactive oxygen species in the cardiovascular system. *Circ Res*. 2015;116(3):531-549. doi:10.1161/CIRCRESAHA.116.303584.Regulation.

91. Chen Y, Gibson SB. Is mitochondrial generation of reactive oxygen species a trigger for autophagy? *Autophagy*. 2008;4(2):246-248. doi:5432 [pii].

92. Filomeni G, De Zio D, Cecconi F. Oxidative stress and autophagy: the clash between damage and metabolic needs. *Cell Death Differ*. 2015;22(3):377-388. doi:10.1038/cdd.2014.150.

93. Wyrsch P, Blenn C, Bader J, Althaus FR. Cell death and autophagy under oxidative stress: roles of poly(ADP-Ribose) polymerases and Ca(2+). *Mol Cell Biol*. 2012;32(17):3541-3553. doi:10.1128/MCB.00437-12.

94. Chen Y, Azad MB, Gibson SB. Superoxide is the major reactive oxygen species regulating autophagy. *Cell Death Differ*. 2009;16(7):1040-1052. doi:10.1038/cdd.2009.49.

95. Carballo M, Conde M, El Bekay R, et al. Oxidative stress triggers STAT3 tyrosine phosphorylation and nuclear translocation in human lymphocytes. *J Biol Chem*. 1999;274(25):17580-17586. doi:10.1074/jbc.274.25.17580.

96. Sobotta MC, Liou W, Stöcker S, et al. Peroxiredoxin-2 and STAT3 form a redox relay for H2O2 signaling. *Nat Chem Biol*. 2014;11(november):1-8. doi:10.1038/nchembio.1695.

97. Ferber EC, Peck B, Delpuech O, Bell GP, East P, Schulze A. FOXO3a regulates reactive oxygen metabolism by inhibiting mitochondrial gene expression. *Cell Death Differ*. 2012;19(6):968-979. doi:10.1038/cdd.2011.179.

98. Gibson SB. Investigating the role of reactive oxygen species in regulating autophagy. In: *Methods in Enzymology*. Vol 528. 1st ed. Elsevier Inc.; 2013:217-235. doi:10.1016/B978-0-12-405881-1.00013-6.

99. Chen L, Xu B, Liu L, et al. Hydrogen peroxide inhibits mTOR signaling by activation of AMPKa leading to apoptosis of neuronal cells. *Lab Investig*. 2010;90(5):762-773. doi:10.1038/labinvest.2010.36.

100. Kongara S, Karantza V. The interplay between autophagy and ROS in tumorigenesis. *Front Oncol*. 2012;2(November):171. doi:10.3389/fonc.2012.00171.

101. Lee G, Won H-S, Lee Y-M, et al. Oxidative Dimerization of PHD2 is Responsible for its Inactivation and Contributes to Metabolic Reprogramming via HIF-1 α Activation. *Sci Rep*. 2016;6(18928):1-12. doi:10.1038/srep18928.

102. Waypa GB, Smith KA, Schumacker PT. O2 sensing, mitochondria and ROS signaling: the fog is lifting. *Mol Aspects Med*. 2016;0:76-89. doi:10.1016/j.mam.2016.01.002.O.

103. Sabharwal SS, Schumacker PT. Mitochondrial ROS in cancer: initiators, amplifiers or an Achilles' heel? *Nat Rev Cancer*. 2014;14(11):709-721. doi:10.1038/nrc3803.Mitochondrial.

104. Castaldo SA, Freitas JR, Conchinha NV, Madureira PA. The Tumorigenic Roles of the Cellular REDOX Regulatory Systems. *Oxid Med Cell Longev*. 2016;2016:1-17. doi:10.1155/2016/8413032.

105. Gupta SC, Hevia D, Patchva S, Park B, Koh W, Aggarwal BB. Upsides and downsides of reactive oxygen species for cancer: the roles of reactive oxygen species in tumorigenesis, prevention, and therapy. *Antioxid Redox Signal*. 2012;16(11):1295-1322. doi:10.1089/ars.2011.4414.

106. Balamurugan K. HIF-1 at the crossroads of hypoxia, inflammation, and cancer. *Int J Cancer*. 2016;138(5):1058-1066. doi:10.1002/ijc.29519.HIF-1.

107. Erkan M, Kleeff J, Esposito I, Giese T, Ketterer K, Buchler MW. Loss of BNIP3 expression is a late event in pancreatic cancer contributing to chemoresistance and worsened prognosis. *Oncogene*. 2005;24:4421-4432. doi:10.1038/sj.onc.1208642.

108. Murai M, Toyota M, Satoh A, et al. Aberrant DNA methylation associated with silencing BNIP3 gene expression in haematopoietic tumours. *Br J Cancer*. 2005;92:1165-1172. doi:10.1038/sj.bjc.6602422.

109. Chourasia AH, Tracy K, Frankenberger C, et al. Mitophagy defects arising from BNip 3 loss promote mammary tumor progression to metastasis. *EMBO Rep*. 2015;16(9):1145-1163.

110. Vijayalingam S, Pillai SG, Rashmi R, Subramanian T, Sagartz JE, Chinnadurai G. Overexpression of BH3-Only Protein BNIP3 Leads to Enhanced Tumor Growth. *Genes Cancer*. 2010;1(9):964-971. doi:10.1177/1947601910386110.

111. Szopa W, Burley TA, Kramer-Marek G, Kaspera W. Diagnostic and Therapeutic Biomarkers in Glioblastoma: Current Status and Future Perspectives. *Biomed Res Int*. 2017;2017:1-13. doi:10.1155/2017/8013575.

112. Huse JT, Holland E, DeAngelis LM. Glioblastoma: Molecular Analysis and Clinical Implications. *Annu Rev Med*. 2012;64(1):121008173401008. doi:10.1146/annurev-med-100711-143028.

113. Alifieris C, Trafalis DT. Glioblastoma multiforme: Pathogenesis and treatment. *Pharmacol Ther*. 2015;152:63-82. doi:10.1016/j.pharmthera.2015.05.005.

114. Bleeker FE, Molenaar RJ, Leenstra S. Recent advances in the molecular understanding of glioblastoma. *J Neurooncol*. 2012;108(1):11-27. doi:10.1007/s11060-011-0793-0.

115. Diwan A, Krenz M, Syed FM, et al. Inhibition of ischemic cardiomyocyte apoptosis through targeted ablation of Bnip3 restrains postinfarction remodeling in mice. *J Clin Invest*. 2007;117(10):2825-2833. doi:10.1172/Table.

116. Rasband WS. ImageJ.

117. Perry SW, Norman JP, Barbieri J, Brown EB, Gelbard HA. Mitochondrial membrane potential probes and the proton gradient: a practical usage guide. *Biotechniques*. 2011;50(2):98-115. doi:10.2144/000113610.Mitochondrial.

118. Perfettini J-L, Roumier T, Kroemer G. Mitochondrial fusion and fission in the control of apoptosis. *Trends Cell Biol*. 2005;15(4):179-183.

119. BOLTE S, CORDELIÈRES FP. A guided tour into subcellular colocalization analysis in light. *J Microsc*. 2006;224(3):213-232.

120. Hanahan D, Weinberg RA. Hallmarks of Cancer: The Next Generation. *Cell*. 2011;144(5):646-674. doi:10.1016/j.cell.2011.02.013.

121. Xu M, Gao X, Ruan C, et al. miR-103 Regulates Oxidative Stress by Targeting the BCL2/Adenovirus E1B 19 kDa Interacting Protein 3 in HUVECs. *Oxid Med Cell Longev*. 2015;2015:1-11. doi:10.1155/2015/489647.

122. Chandel NS, McClintock DS, Feliciano CE, et al. Reactive Oxygen Species Generated at Mitochondrial Complex III Stabilize Hypoxia-inducible Factor-1a during Hypoxia. *J Biol Chem*. 2000;275(33):25130-25138. doi:10.1074/jbc.M001914200.